On the Performance of Spatial Modulation MIMO for Full-Duplex Relay Networks

Sandeep Narayanan, *Member, IEEE*, Hamed Ahmadi, *Senior Member, IEEE*, and Mark F. Flanagan, *Senior Member, IEEE*

***Abstract*—In this paper, we investigate, for the first time, the performance of a full-duplex (FD) relaying protocol, where a single-RF Spatial Modulation (SM) Multiple-Input Multiple-Output (MIMO) system is employed at the relay node. We refer to this protocol as SM-aided FD relaying (SM-FDR). At the destination, a demodulator that takes advantage of the direct connectivity between the source and destination is developed in order to maximize its performance. Based on this demodulator, we introduce a mathematical framework for computing the average error-probability of SM-FDR in the presence of residual Self-Interference (SI). Furthermore, we derive mathematical expressions for computing the achievable rate of SM-FDR. With the aid of these achievable rate expressions, we provide an estimate on the quality of SI cancellation required for the suitability of FD transmission. In addition, we develop and evaluate three relay selection policies specifically designed for the SM-FDR protocol. The mathematical analysis is substantiated with the aid of extensive Monte Carlo simulations. Finally, we also assess the performance of SM-FDR against traditional FD relaying protocols.**

***Index Terms*—Full-Duplex, Relaying, MIMO, Spatial Modulation, Performance Analysis.**

I. Introduction

Relaying has emerged as a strong candidate technology to fulfill, at least in part, the growing data demands of future wireless applications [1]. Furthermore, as recognized by the Third Generation Partnership Projects Long Term Evolution-Advanced (3GPP LTE-A), relaying is an effective way to enhance the coverage and achievable rate at cell edges and in hot spot areas [2]. The most popular relaying protocols available in the literature are amplify-and-forward (AF) and and decode-and-forward (DF) relaying [3]. In spite of their many advantages, one of the fundamental challenges of these relaying protocols is their requirement for extra bandwidth resources due to the half-duplex (HD) constraint of the relay, i.e., the relay cannot transmit and receive on the same frequency at the same time. This might result in a loss of system throughput. Recently, several solutions have been proposed to overcome these limitations [4]. Notable examples include non-orthogonal relaying [5]–[7], successive relaying [8], [9], physical-layer or analog network coding [10], [11], superposition modulation [12], [23], and distributed Spatial Modulation (SM) [14], [15]. In general, these protocols rely on HD relay nodes, and due to practical considerations, discard the possibility of full-duplex (FD) nodes being feasible. More recently, however, promising results on the feasibility of FD transmission have been reported in [16]–[18]. Motivated by this consideration, in the present paper, we focus our attention on FD relaying.

FD transmission capability allows the relays to transmit and receive simultaneously on the same channel, thus effectively doubling the spectral efficiency. However, the success of FD operation is dependent on its capability to suppress the so-called Self-Interference (SI), i.e., the interference introduced from the relay's transmitter to its receiver. In the last few years, several attempts for effectively suppressing the SI have been made. The SI cancellation methods can be broadly classified into two categories [19]: i) *passive cancellation*, which is realized by imposing path-loss between transmit and receive antennas of the relay; and ii) *active cancellation*, which includes analog cancellation techniques, digital cancellation techniques, or a combination of both. A comprehensive survey and assessment of the advantages/disadvantages of these solutions is available in [19, Table 1] and [20], to which the reader is referred for further information. In practice, these cancellation techniques are not capable of fully mitigating SI. Therefore, current works on FD relaying explicitly take into account the effects of imperfect SI cancellation. In particular, the authors of [21] and [22] study the error rate performance of AF-based and DF-based FD relaying, respectively, in the presence of residual SI. In [23] and [24], the authors apply efficient cooperative protocols in an attempt to extract the full benefits of FD relaying. In [25], the authors propose a distributed FD Alamouti scheme that provides significant diversity gains as the strength of the SI decreases. The authors of [26] and [27] propose hybrid relaying schemes that switch opportunistically between FD and HD relaying modes based on a pre-defined criterion. Also, the authors of [26] apply transmit power adaptation for maximizing the spectral efficiency. The authors of [28] investigate several relay selection policies in order to improve the outage probability of FD relaying. In summary, these papers have shown the potential benefits of FD relaying over conventional HD relaying.

SM is an emerging single-RF MIMO concept and a promising candidate for 5G physical-layer technology [29], [30]. SM

Manuscript received May 11, 2016; revised October 24, 2016; and January 05, 2017, accepted March 10, 2017. Date of publication XXXX XX, 2015; date of current version XXXX XX, 2015. This work was supported by Science Foundation Ireland under Grant 13/CDA/2199 and is co-funded under the European Regional Development Fund under Grant Number 13/RC/2077. The editor coordinating the review of this paper and approving it for publication was Prof. Mohamed-Slim Alouini.

S. Narayanan is with the Centre for Telecommunications Research, Department of Informatics, King's College London, London WC2R 2LS, U.K. He was with University College Dublin, Dublin 4, Ireland (e-mail: sandeep.kadanveedu@kcl.ac.uk).

H. Ahmadi and M. F. Flanagan are with with the School of Electrical and Electronic Engineering, University College Dublin, Dublin 4, Ireland (e-mail: hamed.ahmadi@ucd.ie, mark.flanagan@ucd.ie).

introduces a new degree of freedom to convey information, which consists in mapping part of the information to be transmitted into the channel impulse responses of the antenna-array at the transmitter. More specifically, in SM, the data to be transmitted is encoded onto to the conventional signal constellation, i.e., amplitude/phase modulation, as well as onto the new spatial constellation, i.e., the physical location of the single active transmit antenna [32]. Owing to this particular encoding process, recent analytical, simulation and experimental studies have concluded that SM can outperform, with low implementation and computational complexity, many traditional MIMO transmission schemes [33]–[37]. Furthermore, more recent results have highlighted the potential benefits of using SM in a range of application scenarios, such as green cellular networks [38] and massive MIMO [39], [40]. A comprehensive survey of SM is available in [30] and [41], to which the reader is referred for further information. In the present paper, we focus on another application of SM, which is in the context of relay networks. Several researchers have reported encouraging results on SM-based relay-aided protocols. Notable examples include [15], [42], [44], [45], [47] and [48]. In particular, in [15], a distributed SM protocol, which increases the aggregate network throughput by allowing the relays to forward the data of the source while transmitting their own data, has been proposed. In [42], the authors attempt to further enhance the network throughput of distributed SM by allowing the source to transmit in every time-slot. In [44] and [45], space-shift keying [43], which is a low-complexity form of SM, based virtual MIMO systems have been developed for the uplink for cellular networks. In [47], a cooperative space-time shift keying protocol has been proposed, where the relay nodes re-encode the received data from the source onto a dispersion vector and onto a modulated symbol. In [48], an SM-aided detect-and-forward relaying protocol has been proposed. The protocol has been shown to improve the link reliability by identifying the appropriate number of bits to be remodulated at the relays. A summary of other cooperative SM-based protocols are available in [15, Section I], and well as in [30, Section V-B]. These relaying protocols, however, rely on single-/multi-antenna HD relays, and do not explore the potential of FD relays in order to enhance the network performance.

SM is a MIMO technology that is inherently suitable for FD transmission, as the inactive antennas in the antenna-array can be utilized for signal reception, while one of the data-selected antennas is in the transmission mode. The antenna(s) that is in the transmit/receive mode in the current time-slot may change during the next time-slot depending on the incoming data stream. Therefore, the same antennas are adaptively used for transmission and reception of data, thus making the best use of the limited antenna resources. In other words, in traditional SM the inactive antenna(s) intrinsically take part in improving the spectral efficiency of the system, whereas in FD SM, the inactive antenna(s) can be used to improve the spectral efficiency, *as well as* to receive data transmitted from other nodes. In [49], the authors design a novel SI cancellation scheme for FD SM by taking advantage of the reciprocity of the direction of SI signal flow. SM for FD point-to-point transmission has been considered in [50] and [51]. FD SM in the context of relaying systems has been considered in [52]–[55]. Briefly, in [52]–[54], an FD two-way relaying scheme with SM is considered, where two sources communicates with each other using a multi-antenna relay node. In particular, in [52] and [53], the relay node operates in HD mode, and hence the system is free from the effects of SI. In [52] and [54], both the sources are multi-antenna nodes, and the demodulator is built on the assumption that no direct is available between them. Also, the SI channel in [54] is characterized as Rayleigh fading. In [55], an FD relaying system is considered, where the multi-antenna source uses transmit beamforming to forward its data to the relay, and the relay uses SM to forward the data to the destination. However, the effects of SI and the direct link have not been taken into consideration. Against this background, in the present paper, we investigate the performance of a new SM transmission protocol for FD relay networks, and throughout this paper, it is referred to as SM-aided FD relaying (SM-FDR). In simple terms, SM-FDR utilizes a single multi-antenna FD relay to decode, and then forward to the destination using SM, the data symbol transmitted from the source, while simultaneously receiving the source's next transmitted symbol. This helps to significantly improve the aggregate throughput of the network.

The main contributions of this paper can be summarized as follows.

1) An SM-FDR protocol, where an FD relay node with arbitrary number of antennas, N_R, employs single-RF SM to forward the source's data, is investigated and compared with that of traditional FD relaying protocols. We start by developing a demodulator at the destination that takes advantage of the direct connectivity between the source and the destination. In SM-FDR, unlike conventional HD relaying, the source's new symbol is received at the destination through the direct information path *simultaneously* with its previous symbol through the relaying path. The demodulator exploits both signal paths in order to maximize the system performance. It is worth noting that, in prior works on DF based FD protocols, the direct link is either treated as interference, e.g., [26] or it is completely ignored, e.g., [22].
2) We introduce a comprehensive mathematical framework for computing the average error-probability of SM-FDR. The framework takes into account the presence of the direct link to the destination, as well as the presence of SI at the relay node. More specifically, if $N_R = 2$, the framework is developed with the aid of Gil-Pelaez inversion theorem, and is applicable to SI channels with *Rician* fading, which most accurately characterizes the nature of SI [56]. On the other hand, if $N_R > 2$, for analytical tractability, the framework is developed for *Rayleigh* fading on the SI links. In addition, the achievable diversity of SM-FDR is analytically studied. The mathematical approach is new, and can be easily adapted for the analysis of conventional FD relaying as well. The accuracy of the mathematical framework is substantiated with the aid of Monte Carlo simulations.

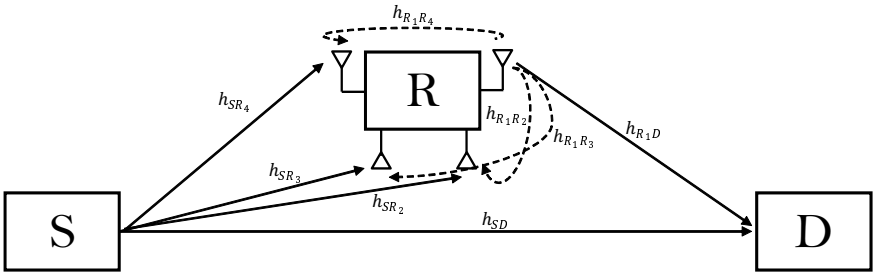

Fig. 1: Illustration of the SM-FDR protocol for $N_R = 4$ and in the presence of residual SI at the relay. The solid lines denote the *useful* channels and the dashed lines denote the SI channels. The index of the active antenna is considered to be $p = 1$.

3) We provide mathematical expressions for computing the instantaneous achievable rate of the SM-FDR protocol. With the aid of these expressions, we derive explicit constraints on the quality of SI cancellation required for SM-FDR to outperform its HD counterpart, SM-aided HD Relaying (SM-HDR).
4) We evaluate three relay selection policies that we developed specifically for SM-FDR. The first and the second policy enhances the instantaneous achievable rate of the system, and exploits the instantaneous Channel State Information (CSI) of the source-to-relay, the relay-to-destination, and the SI channels. The third policy, on the other hand, is used to minimize the instantaneous error-probability, and requires only the instantaneous CSI of the source-to-relay and the relay-to-destination channels.

Notation: $\Pr\{\cdot\}$ denotes probability. $\mathbb{E}_X\{\cdot\}$ denotes the expectation computed with respect to the Random Variable (RV) X. Z^*, $|Z|$ and θ_Z denote denote complex conjugate, absolute value and phase of a complex number Z, respectively. $\mathrm{Re}\{\cdot\}$ and $\mathrm{Im}\{\cdot\}$ denote real and imaginary part operators. $j = \sqrt{-1}$ denotes the imaginary unit. $Q(x) = \left(1/\sqrt{2\pi}\right)\int_x^{+\infty}\exp\left(-t^2/2\right)dt$ denotes the Q-function. $\Gamma(x) = \int_0^{\infty} t^{x-1}\exp(-t)dt$ is the Gamma function.

II. Transmission Protocol

A. System Model

A typical dual-hop, three-node network topology is considered as shown in Fig. 1, where an HD source, S, communicates with its intended HD destination, D, with the aid of an FD relay node, R. The source and the destination are equipped with one antenna each, whereas the relay is equipped with N_R antennas. The FD operation at the relay results in SI, which is suppressed with the aid of some SI cancellation technique as described earlier in Section I. However, the full cancellation of SI is not possible due to practical reasons. Therefore, the quality of the cancellation technique is explicitly taken into account in our work. A direct link also exists between the source and the destination. The demodulator at the destination given in Section II-D takes advantage of the direct link to minimize the error-probability and to enhance the achievable rate.

In SM-FDR, the source broadcasts its data symbol to the relay and the destination. The relay demodulates the data and then forwards it to the destination by using SM. Simultaneously, the source broadcasts a new symbol to the relay and the destination. The SM encoding process enables the relay to restrict its number of active RF transmit chains to just one. This helps to significantly reduce the relay's power consumption [57]. More specifically, one of the N_R antennas is chosen for activation based on SM and the estimated data of the source at the relay. During this activation instance, the remaining $N_R - 1$ antennas at the relay are available for reception of the next symbol from the source.

Employing SM at the relay requires two main considerations. 1) Unlike conventional point-to-point SM, the inactive antenna(s) at the relay in SM-FDR are not switched off. Instead they are switched on in the receive mode. Since the symbols transmitted from the source are equiprobable, the active/inactive antenna(s) in the current time-slot and in the next time-slot may be different. 2) For high data-rate transmission, the RF antenna switching at the relay to enable the simultaneous transmission and the reception of data should be in agreement with symbol-time switching mechanism that is particular to SM. Fortunately, as remarked in [30], high-speed RF switches that serve this purpose with low insertion loss and good isolation properties have been reported in the literature.

B. Channel Model

Quasi-static fading is assumed, which implies that each wireless fading channels remain static over one cooperative phase, *i.e.*, two time-slots, while it changes independently from one cooperative phase to another.

1) The SI channel from the p-th transmit antenna of the relay to its r-th receive antenna, for $r, p \in \{1, 2, ..., N_R\}$, with $p \neq r$ is denoted as $h_{R_pR_r}$, where $h_{R_pR_r} = \left|h_{R_pR_r}\right|\exp\left(j\phi_{R_pR_r}\right)$ with $\left|h_{R_pR_r}\right|$ being the fading envelope and $\phi_{R_pR_r}$ being the channel phase. If $N_R = 2$, the SI fading envelopes are assumed to be independent and follow Rician distribution. The mean $\mu_{R_pR_r}$ and the variance (per dimension) $\sigma^2_{R_pR_r}$ of the SI channels are formulated as follows [23], [51], [58]:

$$\mu_{R_pR_r} = \sqrt{\frac{K_{R_pR_r}\Omega_R}{1+K_{R_pR_r}}} \qquad \sigma^2_{R_pR_r} = \frac{\Omega_R}{1+K_{R_pR_r}} \tag{1}$$

where: i) $K_{R_pR_r}$ is the Rice factor; ii) $\Omega_R = (1/2)\left(E_R/N_0\right)^{-\lambda}$, with E_R being the relay's average transmit energy per symbol, and λ being a small positive constant which captures the quality of SI cancellation. For instance, $\lambda = 0$ implies a poor SI cancellation process, and $\lambda = 1$ refers to a high-quality SI cancellation process. This modeling of SI channels as Rician are in accordance with the recent experimental results reported in [56]. If $N_R > 2$, for the sake of analytical tractability, the SI fading envelopes are assumed to be Rayleigh distributed, i.e., $\mu_{R_pR_r} = 0$, and their channel phases are assumed to be uniformly distributed in $[0, 2\pi]$.

2) The "useful channels", *i.e.*, the source-to-relay, the source-to-destination and the relay-to-destination channels are denoted as h_{SR_r}, h_{SD} and h_{R_pD}, for $r, p \in \{1, 2, ..., N_R\}$, with $r \neq p$. For ease of mathematical analysis, these fading channels are assumed to be independent and to follow a Rayleigh distribution having zero mean and variance (per dimension) $\sigma^2_{SR_r}$, σ^2_{SD} and $\sigma^2_{R_pD}$, respectively. The channel phases follow uniform distribution in $[0, 2\pi]$.

C. Relaying Protocol

During the t-th time-slot, the source broadcasts its data to the relay and the destination. Accordingly, the signal received at the inactive antennas of the relay, and the destination, can be formulated as follows:

$$\begin{cases} y_{SR_r}(t) = \sqrt{E_S} h_{SR_r} x_S(t) + \sqrt{E_R} h_{R_pR_r} x_R(t) + n_{R_r}(t) \\ y_D(t) = \sqrt{E_S} h_{SD} x_S(t) + \sqrt{E_R} h_{R_pD} x_R(t) + n_D(t) \end{cases} \tag{2}$$

where: i) p is the index of the active antenna at relay during the t-th time-slot; ii) $r \in \{1, 2, ..., N_R\} \setminus p$ are the antennas that are in the receive mode during the t-th time-slot; iii) E_S and E_R are the sources and relay's average transmit energy per symbol, respectively; iv) $x_S(t) \in \mathcal{A}_S$ is the M-ary complex modulated symbol transmitted by the source during the t-th time-slot; iv) $x_R(t) \in \mathcal{A}_R$ is the N-ary complex modulated symbol transmitted from the active antenna of the relay during the t-th time-slot. We assume $\mathcal{A}_S$ and $\mathcal{A}_R$ are either Phase Shift Keying (PSK) or Quadrature Amplitude Modulation (QAM) constellations, whose symbols have a power constraint of unity, i.e., $\mathbb{E}\left\{|x_S(\cdot)|^2\right\} = 1$ and $\mathbb{E}\left\{|x_R(\cdot)|^2\right\} = 1$. The active antenna-index p and the symbol $x_R(t)$ are obtained as an outcome of the SM encoding process at the relay. This will become more apparent in the later part of this section; and v) $n_X(t)$ is the complex Additive White Gaussian Noise (AWGN) at the input of node X during the t-th time-slot. The AWGN is independent and identically distributed (i.i.d) with zero mean and variance $N_0/2$ per dimension.

It is worth noting that when $t = 0$, i.e., during the very first instance of transmission of data from the source, the relay does not have any data in its buffer to forward to the destination, and hence, we may write $x_R(0) = 0$. Furthermore, since none of the antennas at the relay are in the active mode during at $t = 0$, all the N_R antennas are available for reception of data. This is in contrast to the rest of the time-slots where only $N_R - 1$ antennas are available. Therefore, at $t = 0$, (2) can be rewritten as follows ($r = 1, 2, ..., N_R$):

$$\begin{cases} y_{SR_r}(0) = \sqrt{E_S} h_{SR_r} x_S(0) + n_{R_r}(0) \\ y_D(0) = \sqrt{E_S} h_{SD} x_S(0) + n_D(0) \end{cases} \tag{3}$$

The destination keeps the received signal $y_D(t)$ in (2) for further processing during the $(t+1)$-th time-slot. The relay, on the other hand, demodulates the received signal using the interference-oblivious Maximum-Likelihood (ML) criterion [58]. Accordingly, the demodulator at the relay can be formulated as follows:

$$\begin{cases} \widehat{x}_S^{(R)}(t) \\ \quad = \min\limits_{\widetilde{x}_S^{(R)}(t) \in \mathcal{A}_S} \left\{ \Lambda^{(R)} = \sum\limits_{\substack{r=1 \\ r \neq p}}^{N_R} \left| y_{SR_r}(t) - \sqrt{E_S} h_{SR_r} \widetilde{x}_S^{(R)}(t) \right|^2 \right\} \\ \widehat{b}_S^{(R)}(t) = \mathcal{B}\left(\widehat{x}_S^{(R)}(t) \right) \end{cases} \tag{4}$$

where: i) $\widehat{x}_S^{(R)}(t)$ and $\widehat{b}_S^{(R)}(t)$ are the estimated symbol and the estimated bits at the relay during the t-th time-slot; ii) $\widetilde{x}_S^{(R)}(t)$ is the trial symbol used in the hypothesis detection problem; and iii) $\mathcal{B}(\cdot)$ is the symbol-to-bits mapping function at the source. This mapping function facilitates the SM encoding at the relay.

During the $(t+1)$-th time-slot, the source broadcasts a new symbol to the relay and the destination. Similarly to (2), the received signal at the r'-th inactive antenna of the relay ($r' \in \{1, 2, ..., N_R\} \setminus p'$), and the destination can be formulated as follows:

$$\begin{cases} y_{SR_{r'}}(t+1) = \sqrt{E_S} h_{SR_{r'}} x_S(t+1) \\ \qquad\qquad + \sqrt{E_R} h_{R_{p'}R_{r'}} x_R(t+1) + n_{R_{r'}}(t+1) \\ y_D(t+1) = \sqrt{E_S} h_{SD} x_S(t+1) \\ \qquad\qquad + \sqrt{E_R} h_{R_{p'}D} x_R(t+1) + n_D(t+1) \end{cases} \tag{5}$$

Equation (5) deserves some comments. 1) The active antenna index p' and the transmitted symbol $x_R(t+1)$ of the relay during the $(t+1)$-th time-slot are determined by its estimated bits $\widehat{b}_S^{(R)}(t)$ during the t-th time-slot. More specifically, $(p', x_R(t+1)) = \mathcal{SM}\left(\widehat{b}_S^{(R)}(t)\right)$, where $\mathcal{SM}(\cdot)$ is the bits-to-SM mapping function, p' is the antenna–index and $x_R(\cdot)$ is the PSK symbol. The SM encoding process is elaborated in detail in [31, Fig. 3], to which the reader is referred for further information. 2) The *dash* notation in p' and r' for active and inactive antennas at the relay during the $(t+1)$-th time-slot are introduced to emphasize that the active/inactive antennas during the t-th and $(t+1)$-th time-slot may be different as the data transmitted from the source are equiprobable.

D. Demodulation at the destination

Two copies of each source's data symbol are received at the destination, during the t-th (via direct link) and $(t+1)$-th time-slot (via the relays using SM). The destination makes use of both of these copies for potential diversity/achievable rate benefits. By applying the ML criterion, the destination,

during the $(t+1)$ time-slot, demodulates the source's data transmitted by it during the t-th time-slot. Accordingly, the demodulator can be formulated as in (6), shown at the bottom of this page, where $\left(p, x_R^{(D)}(t)\right) = \mathcal{SM}\left(\mathcal{B}\left(\widehat{x}_S^{(D)}(t-1)\right)\right)$ and $\left(\widetilde{p}', \widetilde{x}_R^{(D)}(t+1)\right) = \mathcal{SM}\left(\mathcal{B}\left(\widetilde{x}_S^{(D)}(t)\right)\right)$.

Some comments about the demodulator in (6) are worth making here. 1) The demodulation process in (6) occurs during the $(t+1)$-th time-slot. However, the symbol t in the estimate $\widehat{x}_S^{(D)}(t)$ has been retained in order to be explicit that $\widehat{x}_S^{(D)}(t)$ is the estimate of $x_S(t)$. 2) The source's data transmitted during the $(t+1)$-th time-slot, i.e., $x_S(t+1)$, is not estimated during the $(t+1)$-th, although we are searching for it over all the constellation using the trial symbol $\widetilde{x}_S^{(D)}(t+1)$. In fact, the estimation of $x_S(t+1)$ is performed at the destination during the $(t+2)$-th time-slot. 3) The ML demodulator in (6) is sub-optimal in the sense that it is not robust to possible demodulation errors at the relay. The optimal receivers, on the other hand, can be developed using the similar line of thought as in [14]. Such a demodulator, however, is prohibitively complex for higher-order modulation, and requires the knowledge of source-to-relay CSI at the destination, which in general, is hard to obtain. For this reason, and for ease of exposition of our proposed protocol, in this paper we consider only the ML demodulator. The MAP demodulator for SM-FDR is not a trivial extension of the ML demodulator in (6) and can be considered as an interesting future line of research.

In the next section, we analyze the performance of the SM-FDR protocol in terms of error probability.

III. Error Probability Analysis

In this section, we derive closed-form expressions for computing the end-to-end Average Symbol Error Probability (ASEP) of SM-FDR. In general, SM-FDR is a DF-based protocol, as the relay first demodulates the source's data before forwarding it to the destination. Therefore, the end-to-end ASEP at the destination can be formulated as follows [59]:

$$\begin{aligned}\mathrm{ASEP}_{\mathrm{SM-FDR}} = \mathrm{ASEP}^{(SR)}\mathrm{ASEP}_{\mathrm{e}}^{(SRD)} \\ + \left(1 - \mathrm{ASEP}^{(SR)}\right)\mathrm{ASEP}_{\mathrm{c}}^{(SRD)}\end{aligned} \tag{7}$$

where: i) $\mathrm{ASEP}^{(SR)}$ is the ASEP at the relay related to the transmission from the source; ii) $\mathrm{ASEP}_{\mathrm{c}}^{(SRD)}$ is the ASEP at the destination related to the combined transmission from the source and the relay given that the relay demodulated correctly; ii) $\mathrm{ASEP}_{\mathrm{e}}^{(SRD)}$ is the ASEP at the destination given that the relay demodulated incorrectly.

In what follows, we derive closed-form mathematical expressions for each of the ASEP terms in (7). The analytical development of the ASEPs consists of two steps: i) first, the Average Pairwise Error Probability (APEP) is computed; and ii) then, the ASEP is obtained from it with the aid of union-bound or Nearest Neighbor (NN) approximation methods.

A. Computation of $\mathrm{ASEP}^{(SR)}$

1) $\mathrm{APEP}^{(SR)}\left(x_S^{(R)}(t) \to \widetilde{x}_S^{(R)}(t)\right)$ *for* $N_R = 2$*:* We first derive an exact closed-form expression for the computation of $\mathrm{APEP}^{(SR)}$ when $N_R = 2$. In this case, the number of antennas in the receive mode at the relay is $\Omega_{\mathrm{Rx}}^{(R)} = N_R - 1 = 1$. Let $x_S^{(R)}(t)$ be the actual symbol transmitted from the source during the t-th time-slot and $\widetilde{x}_S^{(R)}(t)$ be the hypothesis. Then, the $\mathrm{PEP}^{(SR)}\left(x_S^{(R)}(t) \to \widetilde{x}_S^{(R)}(t)\,|\mathbf{h}^{(R)}, \mathbf{n}^{(R)}\right)$ is defined as the probability of erroneously deciding on the symbol $\widetilde{x}_S^{(R)}(t)$ at the relay node when $x_S^{(R)}(t)$ is the actual symbol transmitted by the source, where we assume that they are the only two symbols possibly being transmitted from the source and that AWGN $\mathbf{n}^{(R)}$ and fading channels $\mathbf{h}^{(R)}$ are fixed [14]. In particular, $\mathbf{h}^{(R)}$ and $\mathbf{n}^{(R)}$ are the short-hands used to denote all fading channels and noises at the relay. In mathematical terms we have:

$$\begin{aligned}&\mathrm{PEP}^{(SR)}\left(x_S^{(R)}(t) \to \widetilde{x}_S^{(R)}(t)\,|\mathbf{h}^{(R)}, \mathbf{n}^{(R)}\right) \\ &= \Pr\left\{\Lambda^{(R)}\left(\widetilde{x}_S^{(R)}(t)\right) < \Lambda^{(R)}\left(x_S^{(R)}(t)\right)|\mathbf{h}^{(R)}, \mathbf{n}^{(R)}\right\} \\ &\overset{(a)}{=} \Pr\left\{\mathrm{Re}\left\{\left(\sqrt{E_R}h_{RR}x_R(t) + n_R(t)\right)h_{SR}{}^{*}\Delta_S^{(R)*}\right\}\right. \\ &\qquad \left. < -(1/2)\sqrt{E_S}|h_{SR}|^2\left|\Delta_S^{(R)}(t)\right|^2\right\} \\ &\overset{(b)}{=} \Pr\left\{\mathrm{Re}\left\{\left(\sqrt{E_R}h_{RR}x_R(t)\right)\exp\left\{-j\left(\theta_{h_{SR}} + \theta_{\Delta_S^{(R)}(t)}\right)\right\}\right.\right. \\ &\qquad \left.\left. + n_R(t)\right\} < -(1/2)\sqrt{E_S}\,|h_{SR}|\left|\Delta_S^{(R)}(t)\right|\right\}\end{aligned} \tag{8}$$

where: i) $\Delta_S^{(R)}(t) = x_S^{(R)}(t) - \widetilde{x}_S^{(R)}(t)$; ii) (a) follows using the expression of decision metric given in (4), and with the aid of some algebra; and iii) (b) holds because $n_R(t)$ is a circularly symmetric RV. It should be noted that the subscript 'r' has been dropped in (8), as there is only one antenna that is in the receive mode at the relay.

In (8), the SI channel h_{RR} is subject to Rician fading and hence, is not circularly symmetric. In order to proceed further, we express h_{RR} as the sum of a circularly symmetric Gaussian

$$\begin{cases}\widehat{x}_S^{(D)}(t) = \underset{\substack{\widetilde{x}_S^{(D)}(t)\in\mathcal{A}_S \\ \widetilde{x}_S^{(D)}(t+1)\in\mathcal{A}_S}}{\arg\min} \left\{\Lambda^{(D)}\left(\widetilde{x}_S^{(D)}(t), \widetilde{x}_S^{(D)}(t+1)\right)\right\} \\ \Lambda^{(D)}\left(\widetilde{x}_S^{(D)}(t), \widetilde{x}_S^{(D)}(t+1)\right) = \left|y_D(t) - \left(\sqrt{E_S}h_{SD}\widetilde{x}_S^{(D)}(t) + \sqrt{E_R}h_{R_pD}x_R^{(D)}(t)\right)\right|^2 \\ \qquad\qquad + \left|y_D(t+1) - \left(\sqrt{E_S}h_{SD}\widetilde{x}_S^{(D)}(t+1) + \sqrt{E_R}h_{R_{\widetilde{p}'}D}\widetilde{x}_R^{(D)}(t+1)\right)\right|^2\end{cases} \tag{6}$$

RV, $\overline{h}_{RR}$, and a constant, μ_{RR}. In fact, μ_{RR} is the mean of h_{RR}. Therefore, with the aid of (8), we obtain:

$$\begin{aligned}
&\mathrm{PEP}^{(SR)}\left(x_S^{(R)}(t)\to\widetilde{x}_S^{(R)}(t)\,|\mathbf{h}^{(R)},\mathbf{n}^{(R)}\right)\\
&\overset{(a)}{=}\Pr\Big\{\sqrt{E_R}\,|x_R(t)|\,\mathrm{Re}\left\{\overline{h}_{RR}\right\}\\
&\quad+\sqrt{E_R}\,|x_R(t)|\,\mu_{RR}\cos\left(\theta_{h_{SR}}+\overline{\theta}_R\right)+\mathrm{Re}\left\{n_R(t)\right\}\\
&\quad<-(1/2)\sqrt{E_S}\,|h_{SR}|\left|\Delta_S^{(R)}(t)\right|\Big\}\\
&\overset{(b)}{=}\mathcal{F}_{\overline{I}_R+\overline{n}_R}\left(-(1/2)\sqrt{E_S}\,|h_{SR}|\left|\Delta_S^{(R)}(t)\right|\right)\\
&\overset{(c)}{=}\mathrm{PEP}^{(SR)}\left(x_S^{(R)}(t)\to\widetilde{x}_S^{(R)}(t)\,|\,|h_{SR}|,\theta_{h_{SR}},\overline{h}_{RR},\overline{n}_R\right)
\end{aligned}\tag{9}$$

where: i) $\overline{\theta}_R=\theta_{\Delta_S^{(R)}(t)}-\theta_{x_R(t)}$, with $\theta_{x_R(t)}$ being the phase of $x_R(t)$; ii) (a) follows by exploiting the circular symmetry of the RV $\overline{h}_{RR}$; iii) (b) follows from the definition of Cumulative Distribution Function (CDF), with $\overline{I}_R=\sqrt{E_R}\,|x_R(t)|\,\mathrm{Re}\left\{\overline{h}_{RR}\right\}+\sqrt{E_R}\,|x_R(t)|\,\mu_{RR}\cos\left(\overline{\theta}_R\right)$ and $\overline{n}_R=\mathrm{Re}\left\{n_R(t)\right\}$; and iv) (c) explicitly shows the specific RVs on which $\mathrm{PEP}^{(SR)}$ is conditioned.

By using Gil-Palaez inversion theorem [60], the CDF $\mathcal{F}_{\overline{I}_R+\overline{n}_R}(\cdot)$ of (III-A1) can be expressed in terms of its characteristic function (CF), $\Phi_{\overline{I}_R+\overline{n}_R}(\cdot)$ as follows:

$$\begin{aligned}
&\mathrm{PEP}^{(SR)}\left(x_S^{(R)}(t)\to\widetilde{x}_S^{(R)}(t)\,|\,|h_{SR}|,\theta_{h_{SR}},\overline{h}_{RR},\overline{n}_R\right)\\
&=\frac{1}{2}+\frac{1}{\pi}\int_0^\infty\sin\left(-(1/2)\sqrt{E_S}\,|h_{SR}|\left|\Delta_S^{(R)}(t)\right|\omega\right)\omega^{-1}\\
&\qquad\times\Phi_{\overline{I}_R+\overline{n}_R}(\omega)\,d\omega\\
&\overset{(a)}{=}\frac{1}{2}-\frac{1}{\pi}\int_0^\infty\sin\left((1/2)\sqrt{E_S}\,|h_{SR}|\left|\Delta_S^{(R)}(t)\right|\omega\right)\omega^{-1}\\
&\qquad\times\Phi_{\overline{I}_R}(\omega)\,\Phi_{\overline{n}_R}(\omega)\,d\omega\\
&\overset{(b)}{=}\frac{1}{2}-\frac{1}{\pi}\int_0^\infty\sin\left((1/2)\sqrt{E_S}\,|h_{SR}|\left|\Delta_S^{(R)}(t)\right|\omega\right)\omega^{-1}\\
&\qquad\times\left[\Phi_{\overline{n}_R}(\omega)-\Phi_{\overline{n}_R}(\omega)\left(1-\Phi_{\overline{I}_R}(\omega)\right)\right]d\omega\\
&\overset{(c)}{=}\mathrm{PEP}_{\mathrm{N}}^{(SR)}\left(x_S^{(R)}(t)\to\widetilde{x}_S^{(R)}(t)\,|\,|h_{SR}|,\overline{n}_R\right)\\
&\quad+\mathrm{PEP}_{\mathrm{NI}}^{(SR)}\left(x_S^{(R)}(t)\to\widetilde{x}_S^{(R)}(t)\,|\,|h_{SR}|,\theta_{h_{SR}},\overline{h}_{RR},\overline{n}_R\right)
\end{aligned}\tag{10}$$

where: i) (a) follows by noting that $\sin(-x)=-\sin(x)$, and that $\overline{I}_R$ and $\overline{n}_R$ are independent RVs; ii) (b) follows from [61], [62]; and iii) $\mathrm{PEP}_{\mathrm{N}}^{(SR)}(\cdot)$ and $\mathrm{PEP}_{\mathrm{NI}}^{(SR)}(\cdot)$ in (c) are defined as in (11), shown at the bottom of this page.

Note that $\mathrm{PEP}_{\mathrm{N}}^{(SR)}(\cdot)$ is conditioned only on the AWGN and the Rayleigh fading envelope. Whereas, $\mathrm{PEP}_{\mathrm{NI}}^{(SR)}(\cdot)$, in addition to the AWGN and the Rayleigh fading envelope, is also conditioned on the SI channel, as well as the uniformly distributed phase of the source-to-relay channel.

From (10) and (11), the $\mathrm{APEP}^{(SR)}\left(x_S^{(R)}(t)\to\widetilde{x}_S^{(R)}(t)\right)$ can be computed by taking the expectation as in (12), shown at the bottom of this page.

The $\mathrm{APEP}_{\mathrm{N}}^{(SR)}\left(x_S^{(R)}(t)\to\widetilde{x}_S^{(R)}(t)\right)$ of (12) can be computed in closed-form as follows:

$$\begin{aligned}
&\mathrm{APEP}_{\mathrm{N}}^{(SR)}\left(x_S^{(R)}(t)\to\widetilde{x}_S^{(R)}(t)\right)\\
&\overset{(a)}{=}\mathbb{E}_{|h_{SR}|}\left\{Q\left(\sqrt{\frac{E_S}{2N_0}|h_{SR}|^2\left|\Delta_S^{(R)}(t)\right|^2}\right)\right\}\\
&\overset{(b)}{=}\frac{1}{2}\left(1-\sqrt{\frac{(\overline{\gamma}_{SR}/4)\left|\Delta_S^{(R)}(t)\right|^2}{1+(\overline{\gamma}_{SR}/4)\left|\Delta_S^{(R)}(t)\right|^2}}\right)
\end{aligned}\tag{13}$$

where $\overline{\gamma}_{SR}=2\sigma_{SR}^2(E_S/N_0)$, and (a) and (b) follows from [15, Eq. 7] and [15, Eq. 29], respectively.

On the other hand, the closed-form expression for $\mathrm{APEP}_{\mathrm{NI}}^{(SR)}\left(x_S^{(R)}(t)\to\widetilde{x}_S^{(R)}(t)\right)$ is derived in Appendix I.

$$\begin{aligned}
\mathrm{PEP}_{\mathrm{N}}^{(SR)}\left(x_S^{(R)}(t)\to\widetilde{x}_S^{(R)}(t)\,|\,|h_{SR}|,\overline{n}_R\right)&=\frac{1}{2}-\frac{1}{\pi}\int_0^\infty\sin\left((1/2)\sqrt{E_S}\,|h_{SR}|\left|\Delta_S^{(R)}(t)\right|\omega\right)\omega^{-1}\Phi_{\overline{n}_R}(\omega)\,d\omega\\
\mathrm{PEP}_{\mathrm{NI}}^{(SR)}\left(x_S^{(R)}(t)\to\widetilde{x}_S^{(R)}(t)\,|\,|h_{SR}|,\theta_{h_{SR}},\overline{h}_{RR},\overline{n}_R\right)&=\frac{1}{\pi}\int_0^\infty\sin\left((1/2)\sqrt{E_S}\,|h_{SR}|\left|\Delta_S^{(R)}(t)\right|\omega\right)\omega^{-1}\Phi_{\overline{n}_R}(\omega)\\
&\qquad\times\left(1-\Phi_{\overline{I}_R}(\omega)\right)d\omega
\end{aligned}\tag{11}$$

$$\begin{aligned}
\mathrm{APEP}^{(SR)}\left(x_S^{(R)}(t)\to\widetilde{x}_S^{(R)}(t)\right)&=\mathbb{E}_{|h_{SR}|,\overline{n}_R}\left\{\mathrm{PEP}_{\mathrm{N}}^{(SR)}\left(x_S^{(R)}(t)\to\widetilde{x}_S^{(R)}(t)\,|\,|h_{SR}|,\overline{n}_R\right)\right\}\\
&\quad+\mathbb{E}_{|h_{SR}|,\theta_{h_{SR}},\overline{h}_{RR},\overline{n}_R}\left\{\mathrm{PEP}_{\mathrm{NI}}^{(SR)}\left(x_S^{(R)}(t)\to\widetilde{x}_S^{(R)}(t)\,|\,|h_{SR}|,\theta_{h_{SR}},\overline{h}_{RR},\overline{n}_R\right)\right\}\\
&=\mathrm{APEP}_{\mathrm{N}}^{(SR)}\left(x_S^{(R)}(t)\to\widetilde{x}_S^{(R)}(t)\right)+\mathrm{APEP}_{\mathrm{NI}}^{(SR)}\left(x_S^{(R)}(t)\to\widetilde{x}_S^{(R)}(t)\right)
\end{aligned}\tag{12}$$

The final expression is provided below:

$$\begin{cases} \mathrm{APEP}_{\mathrm{NI}}^{(SR)}\left(x_S^{(R)}(t)\to\widetilde{x}_S^{(R)}(t)\right)=\sqrt{\mathcal{I}_1}\left(\Upsilon_1-\Upsilon_2\right) \\ \Upsilon_1=\dfrac{1}{2\sqrt{\mathcal{I}_1+(N_0/4)}} \\ \Upsilon_2=\dfrac{\exp\left(-\frac{E_R|x_R(t)|^2\mu_{RR}^2}{8(\mathcal{I}_1+\mathcal{I}_2+(N_0/4))}\right)\mathrm{I}_0\left(\frac{E_R|x_R(t)|^2\mu_{RR}^2}{8(\mathcal{I}_1+\mathcal{I}_2+(N_0/4))}\right)}{2\sqrt{\mathcal{I}_1+\mathcal{I}_2+(N_0/4)}} \\ \mathcal{I}_1=\dfrac{E_S\left|\Delta_S^{(R)}(t)\right|^2\sigma_{SR}^2}{16};\quad \mathcal{I}_2=\dfrac{E_R|x_R(t)|^2\sigma_{RR}^2}{4} \end{cases} \tag{14}$$

where $\mathrm{I}_0(\cdot)$ denote the zero-order modified Bessel function of the first kind.

It is worth noting here that a closed-form expression for the ASEP of the source-to-relay link in conventional FD relay networks is available in [22]. However, the expression in [22] is only applicable to binary modulation schemes. Furthermore, and more importantly, the framework in [22] is not applicable to Rician SI channels.

2) $\mathrm{APEP}^{(SR)}\left(x_S^{(R)}(t)\to\widetilde{x}_S^{(R)}(t)\right)$ *for* $N_R>2$*:* For the case with $N_R>2$, the computation of $\mathrm{APEP}^{(SR)}\left(x_S^{(R)}(t)\to\widetilde{x}_S^{(R)}(t)\right)$ for Rician SI channels is mathematically difficult. Therefore, for analytical tractability, Rayleigh fading is considered., i.e., $K_{R_pR_r}=0$ for $p,r\in\{1,2,...,N_R\}$, with $p\neq r$. Based on the decision metric in (6), $\mathrm{APEP}^{(SR)}\left(x_S^{(R)}(t)\to\widetilde{x}_S^{(R)}(t)\right)$ can be formulated as follows:

$$\begin{aligned} &\mathrm{APEP}^{(SR)}\left(x_S^{(R)}(t)\to\widetilde{x}_S^{(R)}(t)\right) \\ &=\mathbb{E}_{h_{SR_r}}\left\{Q\left(\sqrt{\sum_{r\in\Omega_{\mathrm{Rx}}^{(R)}}\frac{E_S|h_{SR_r}|^2\left|\Delta_S^{(R)}(t)\right|^2}{2\left(N_0+2E_R|x_R(t)|^2\sigma_{RR}^2\right)}}\right)\right\} \\ &\overset{(a)}{=}\frac{1}{\pi}\prod_{r\in\Omega_{\mathrm{Rx}}^{(R)}}\int_0^{\pi/2}\left(\frac{\sin^2(\theta)}{\sin^2(\theta)+\mathcal{K}_{SR}}\right) \\ &\overset{(b)}{=}\left(\frac{1-\zeta_{SR}}{2}\right)^{N_R-1}\sum_{k=0}^{N_R-2}\binom{N_R-2+k}{k}\left(\frac{1+\zeta_{SR}}{2}\right)^k \end{aligned} \tag{15}$$

where: i) $\mathcal{K}_{SR}=\frac{E_S\sigma_{SR}^2\left|\Delta_S^{(R)}(t)\right|^2}{2\left(N_0+2E_R|x_R(t)|^2\sigma_{RR}^2\right)}$; ii) (a) follows by applying Craig's formula [58, Eq. (4.2)], and then solving the expectation with respect to channel fading; iii) (b) follows from [58, 5A.58], with $\zeta_{SR}=\sqrt{\frac{\mathcal{K}_{SR}}{1+\mathcal{K}_{SR}}}$. Also, we let $\sigma_{SR_r}^2=\sigma_{SR}^2$ and $\sigma_{R_pR_r}^2=\sigma_{RR}^2$, for $r,p\in\{1,2,...,N_R\}$ with $r\neq p$.

Finally, with the aid of the NN approximation, $\mathrm{ASEP}^{(SR)}$ can be formulated as follows [61], [66]:

$$\mathrm{ASEP}^{(SR)}\approx N_{\Delta_{\min}}^{(SR)}\mathrm{APEP}^{(SR)}\left(\left|\Delta_{\min}^{(SR)}\right|\right) \tag{16}$$

where $\left|\Delta_{\min}^{(SR)}\right|=\min_{x_S^{(R)}(t),\widetilde{x}_S^{(R)}(t)\in\mathcal{A}_S}\left\{\left|x_S^{(R)}(t)-\widetilde{x}_S^{(R)}(t)\right|\right\}$, with $x_S^{(R)}(t)\neq\widetilde{x}_S^{(R)}(t)$, is the minimum Euclidean distance among all pairs $\left(x_S^{(R)}(t),\widetilde{x}_S^{(R)}(t)\right)$ of symbols of the constellation $\mathcal{A}_S$, and $N_{\Delta_{\min}}^{(SR)}$ is the average number of nearest neighbors in $\mathcal{A}_S$. Based on the guidelines in [61], for PSK modulation, $\left|\Delta_{\min}^{(SR)}\right|=2\sin(\pi/M)$ with $N_{\Delta_{\min}}^{(SR)}=1$ if $M=2$, and $N_{\Delta_{\min}}^{(SR)}=2$ if $M>2$. For standard square QAM with $M=16$, $\left|\Delta_{\min}^{(SR)}\right|=2/\sqrt{10}$ and $N_{\Delta_{\min}}^{(SR)}=3$.

B. Computation of $\mathrm{ASEP}_c^{(SRD)}$

Let $\mathbf{x}_S^{(D)}=\left(x_S^{(D)}(t),x_S^{(D)}(t+1)\right)$ and $\widetilde{\mathbf{x}}_S^{(D)}=\left(\widetilde{x}_S^{(D)}(t),\widetilde{x}_S^{(D)}(t+1)\right)$ be transmitted and hypothesized symbol vectors. Then, the PEP conditioned on AWGN and fading channels can be formulated as follows:

$$\begin{aligned} &\mathrm{PEP}_{\mathrm{c}}^{(SRD)}\left(\mathbf{x}_S^{(D)}\to\widetilde{\mathbf{x}}_S^{(D)}|\mathbf{h}^{(D)},\mathbf{n}^{(D)}\right) \\ &=\Pr\left\{\Lambda^{(D)}\left(\widetilde{\mathbf{x}}_S^{(D)}\right)<\Lambda^{(D)}\left(\mathbf{x}_S^{(D)}\right)|\mathbf{h}^{(D)},\mathbf{n}^{(D)}\right\} \end{aligned} \tag{17}$$

where $\mathbf{h}^{(D)}$ and $\mathbf{n}^{(D)}$ are the short-hands used to denote all fading channels and noises at the destination.

Remark 1: As evident from (6) and as commented in Section II-D, the decision variable at the destination requires the knowledge of the active antenna index p and the transmitted symbol $x_R^{(D)}(t)$ of the relay at the destination. By noting $\left(p,x_R^{(D)}(t)\right)=\mathcal{SM}\left(\mathcal{B}\left(\hat{x}_S^{(D)}(t-1)\right)\right)$, means that p and $x_R^{(D)}(t)$ are a function of the symbol estimated at the destination during the previous, i.e., $(t-1)$-th time-slot. For the convenience of mathematical analysis, we introduce an approximation that is accurate for high SNR. More specifically, we assume $\hat{x}_S^{(D)}(t-1)=x_S^{(D)}(t-1)$, which implies that the destination has successfully estimated the source's symbol during the $(t-1)$-th time-slot. The accuracy of the proposed approximation is validated by comparing the analytical results against Monte Carlo simulation results in Section VI[1]. The obtained tightness justifies its use in evaluating the ASEP of the SM-FDR protocol.

By using the aforementioned high-SNR approximation and with the aid of some algebra, $\mathrm{PEP}_{\mathrm{c}}^{(SRD)}(\cdot)$ can be simplified as follows:

$$\begin{aligned} &\mathrm{PEP}_{\mathbf{c}}^{(SRD)}\left(\mathbf{x}_S^{(D)}\to\widetilde{\mathbf{x}}_S^{(D)}|\mathbf{h}^{(D)},\mathbf{n}^{(D)}\right) \\ &=\left\{2\mathrm{Re}\left\{\sqrt{E_S}h_{SD}\Delta_S^{(D)}(t)\,n_D(t)^*\right\}\right. \\ &+2\mathrm{Re}\left\{\sqrt{E_S}h_{SD}\Delta_S^{(D)}(t+1)+\left(\sqrt{E_R}h_{R_{p'}D}x_R^{(D)}(t+1)\right.\right. \\ &\left.\left.-\sqrt{E_R}h_{R_{\widetilde{p}'}D}\widetilde{x}_R^{(D)}(t+1)\right)n_D(t+1)^*\right\}\Bigg\} \\ &<-\left|\sqrt{E_S}h_{SD}\Delta_S^{(D)}(t)\right|^2-\left|\sqrt{E_S}h_{SD}\Delta_S^{(D)}(t+1)+\right. \\ &\left.\sqrt{E_R}h_{R_{p'}D}x_R^{(D)}(t+1)-\sqrt{E_R}h_{R_{\widetilde{p}'}D}\widetilde{x}_R^{(D)}(t+1)\right|^2 \end{aligned} \tag{18}$$

[1]In addition to the results in Section VI, the interested reader may also further validate the approximation by plotting the Monte Carlo simulation results for $\mathrm{ASEP}_c^{(SRD)}$ with the approximation $\hat{x}_S^{(D)}(t-1)=x_S^{(D)}(t-1)$ and without this approximation. It can be observed that the approximation is very tight particularly in the high-SNR regime.

where $\Delta_S^{(D)}(k) = x_S^{(D)}(k) - x_S^{(D)}(k)$, for $k = t, t+1$.

With the aid of some algebraic manipulations, (18) can be re-written as in (19), shown at the bottom of this page, where (a) follows from [58, Eq. (4.2)]. On the other hand, $\mathrm{APEP}_{\mathrm{c}}^{(SRD)}\left(\mathbf{x}_S^{(D)} \to \widetilde{\mathbf{x}}_S^{(D)}\right)$ can be formulated by averaging over all fading channels as in (20), shown at the bottom of this page, where: i) (a) follows by exploiting the independence of source-to-destination and relay-to-destination channels. Here we introduce $\mathbf{h}_{RD}$ as a short-hand for all the relay-to-destination channels; and ii) (b) follows by solving the expectation with respect to h_{SD} and with the aid of some simplifications, where we define $\mathcal{K}_{SD} = \bar{\gamma}_{SD}\left(\left|\Delta_S^{(D)}(t)\right|^2 + \left|\Delta_S^{(D)}(t+1)\right|^2\right)$, with $\bar{\gamma}_{SD} = 2(E_S/N_0)\sigma_{SD}^2$, and $\mathcal{K}_{RD} = (E_R/N_0)\,\mathbb{E}_{\mathbf{h}_{RD}}\left\{\left|h_{R_{p'}D}x_R^{(D)}(t+1) - h_{R_{\widetilde{p'}}D}\widetilde{x}_R^{(D)}(t+1)\right|^2\right\}$.

The expectation with respect to $\mathbf{h}_{RD}$ in $\mathcal{K}_{RD}$ can be solved as follows:

$$\mathcal{K}_{RD} = \begin{cases} (E_R/N_0)\left|x_R^{(D)}(t+1) - \widetilde{x}_R^{(D)}(t+1)\right|^2 \mathbb{E}_{h_{R_{p'}D}}\left\{\left|h_{R_{p'}D}\right|^2\right\} \\ \qquad \text{if} \quad p' = \widetilde{p'} \quad \text{and} \quad x_R^{(D)}(t+1) \neq \widetilde{x}_R^{(D)}(t+1) \\ (E_R/N_0)\left|x_R^{(D)}(t+1)\right|^2 \mathbb{E}_{\mathbf{h}_{RD}}\left\{\left|h_{R_{p'}D} - h_{R_{\widetilde{p'}}D}\right|^2\right\} \\ \qquad \text{if} \quad p' \neq \widetilde{p'} \quad \text{and} \quad x_R^{(D)}(t+1) = \widetilde{x}_R^{(D)}(t+1) \\ (E_R/N_0)\,\mathbb{E}_{\mathbf{h}_{RD}}\left\{\left|h_{R_{p'}D}x_R^{(D)}(t+1) - h_{R_{\widetilde{p'}}D}\widetilde{x}_R^{(D)}(t+1)\right|^2\right\} \\ \qquad \text{if} \quad p' \neq \widetilde{p'} \quad \text{and} \quad x_R^{(D)}(t+1) \neq \widetilde{x}_R^{(D)}(t+1) \end{cases}$$

$$\overset{(a)}{=} \begin{cases} 2(E_R/N_0)\left|\Delta_R^{(D)}(t+1)\right|^2 \sigma_{R_{p'}D}^2 \\ \qquad \text{if} \quad p' = \widetilde{p'} \quad \text{and} \quad x_R^{(D)}(t+1) \neq \widetilde{x}_R^{(D)}(t+1) \\ 2(E_R/N_0)\left|x_R^{(D)}(t+1)\right|^2\left(\sigma_{R_{p'}D}^2 + \sigma_{R_{\widetilde{p'}}D}^2\right) \\ \qquad \text{if} \quad p' \neq \widetilde{p'} \quad \text{and} \quad x_R^{(D)}(t+1) = \widetilde{x}_R^{(D)}(t+1) \\ 2(E_R/N_0)\left(\left|x_R^{(D)}(t+1)\right|^2\sigma_{R_{p'}D}^2 + \left|\widetilde{x}_R^{(D)}(t+1)\right|^2\sigma_{R_{\widetilde{p'}}D}^2\right) \\ \qquad \text{if} \quad p' \neq \widetilde{p'} \quad \text{and} \quad x_R^{(D)}(t+1) \neq \widetilde{x}_R^{(D)}(t+1) \end{cases} \tag{21}$$

where $\Delta_R^{(D)}(t+1) = x_R^{(D)}(t+1) - \widetilde{x}_R^{(D)}(t+1)$, and (a) follows by exploiting the independence of $h_{R_{p'}D}$ and $h_{R_{\widetilde{p'}}D}$.

By letting $\sigma_{R_{p'}D}^2 = \sigma_{R_{\widetilde{p'}}D}^2 = \sigma_{R_pD}^2$, for $p', \widetilde{p'} \in \{1, 2, ..., N_R\}$, and by letting $\overline{\gamma}_{R_pD} = 2(E_R/N_0)\sigma_{R_pD}^2$, we obtain:

$$\mathcal{K}_{RD} = 2\overline{\gamma}_{R_pD}\rho_R(t+1) \tag{22}$$

where $\rho_R(t+1) = (1/2)\left|\Delta_R^{(D)}(t+1)\right|^2$ if $p' = \widetilde{p'}$ and $x_R^{(D)}(t+1) \neq \widetilde{x}_R^{(D)}(t+1)$; $\rho_R(t+1) = \left|x_R^{(D)}(t+1)\right|^2$ if $p' \neq \widetilde{p'}$ and $x_R^{(D)}(t+1) = \widetilde{x}_R^{(D)}(t+1)$; and $\rho_R(t+1) = (1/2)\left|x_R^{(D)}(t+1)\right|^2 + (1/2)\left|\widetilde{x}_R^{(D)}(t+1)\right|^2$ if $p' \neq \widetilde{p'}$ and $x_R^{(D)}(t+1) \neq \widetilde{x}_R^{(D)}(t+1)$

By inserting (22) in (20), we get the final expression for $\mathrm{ASEP}_{\mathrm{c}}^{(SRD)}\left(\mathbf{x}_S^{(D)} \to \widetilde{\mathbf{x}}_S^{(D)}\right)$. The integral in (20) can be solved by using [58, Eq. (5A.4b)] and [58, Eq. (5A.75)]. More

$$\begin{aligned} &\mathrm{PEP}_{\mathrm{c}}^{(SRD)}\left(\mathbf{x}_S^{(D)} \to \widetilde{\mathbf{x}}_S^{(D)} | \mathbf{h}^{(D)}\right) \\ &= Q\left(\sqrt{\frac{\left|\sqrt{E_S}h_{SD}\Delta_S^{(D)}(t)\right|^2 + \left|\sqrt{E_S}h_{SD}\Delta_S^{(D)}(t+1) + \sqrt{E_R}h_{R_{p'}D}x_R^{(D)}(t+1) - \sqrt{E_R}h_{R_{\widetilde{p'}}D}\widetilde{x}_R^{(D)}(t+1)\right|^2}{2N_0}}\right) \\ &\overset{(a)}{=} \frac{1}{\pi}\int_0^{\pi/2} \exp\left(-\frac{\left|\sqrt{E_S}h_{SD}\Delta_S^{(D)}(t)\right|^2 + \left|\sqrt{E_S}h_{SD}\Delta_S^{(D)}(t+1) + \sqrt{E_R}h_{R_{p'}D}x_R^{(D)}(t+1) - \sqrt{E_R}h_{R_{\widetilde{p'}}D}\widetilde{x}_R^{(D)}(t+1)\right|^2}{4N_0\sin^2(\theta)}\right) d\theta \end{aligned} \tag{19}$$

$$\begin{aligned} \mathrm{APEP}_{\mathrm{c}}^{(SRD)}\left(\mathbf{x}_S^{(D)} \to \widetilde{\mathbf{x}}_S^{(D)}\right) &\overset{(a)}{=} \frac{1}{\pi}\int_0^{\pi/2} \mathbb{E}_{h_{SD}}\left\{\exp\left(-\frac{E_S|h_{SD}|^2\left(\left|\Delta_S^{(D)}(t)\right|^2 + \left|\Delta_S^{(D)}(t+1)\right|^2\right)}{4N_0\sin^2(\theta)}\right)\right\} \\ &\quad \times \mathbb{E}_{\mathbf{h}_{RD}}\left\{\exp\left(-\frac{E_R\left|h_{R_{p'}D}x_R^{(D)}(t+1) - h_{R_{\widetilde{p'}}D}\widetilde{x}_R^{(D)}(t+1)\right|^2}{4N_0\sin^2(\theta)}\right)\right\} d\theta \\ &\overset{(b)}{=} \frac{1}{\pi}\int_0^{\pi/2}\left(\frac{\sin^2(\theta)}{\sin^2(\theta) + (\mathcal{K}_{SD}/4)}\right)\left(\frac{\sin^2(\theta)}{\sin^2(\theta) + (\mathcal{K}_{RD}/4)}\right) d\theta \end{aligned} \tag{20}$$

specifically, if $\mathcal{K}_{SD}=\mathcal{K}_{RD}=\mathcal{K}$, we obtain:

$$\begin{aligned}&\mathrm{APEP}_{\mathrm{c}}^{(SRD)}\left(\mathbf{x}_S^{(D)}\rightarrow\widetilde{\mathbf{x}}_S^{(D)}\right)\\&=\left(\frac{1-\Psi\left(\mathcal{K}\right)}{2}\right)^2\sum_{\mathcal{K}=0}^{1}\left[\binom{\mathcal{K}+1}{\mathcal{K}}\left(\frac{1+\Psi\left(\mathcal{K}\right)}{2}\right)^{\mathcal{K}}\right]\end{aligned}\tag{23}$$

where $\Psi\left(\mathcal{K}\right)=\sqrt{\frac{\mathcal{K}/4}{1+\mathcal{K}/4}}$.

On the other hand, if $\mathcal{K}_{SD}\neq\mathcal{K}_{RD}$, then $\mathrm{ASEP}_{\mathrm{c}}^{(SRD)}\left(\mathbf{x}_S^{(D)}\rightarrow\widetilde{\mathbf{x}}_S^{(D)}\right)$ reduces to:

$$\begin{aligned}&\mathrm{APEP}_{\mathrm{c}}^{(SRD)}\left(\mathbf{x}_S^{(D)}\rightarrow\widetilde{\mathbf{x}}_S^{(D)}\right)=\frac{1}{2}\left(\frac{\mathcal{K}_{SD}-\mathcal{K}_{RD}}{\mathcal{K}_{SD}}\right)^2\\&\times\left[\left(1-\sqrt{\frac{\mathcal{K}_{SD}/4}{1+\mathcal{K}_{SD}/4}}\right)-\left(1-\sqrt{\frac{\mathcal{K}_{RD}/4}{1+\mathcal{K}_{RD}/4}}\right)\right]\end{aligned}\tag{24}$$

Based on (23) and (24), and by noting that our symbol of interest in the current time-slot is $x_S^{(D)}$, the $\mathrm{ASEP}_{\mathrm{c}}^{(SRD)}$ can be formulated using the union bound as in (25), shown at the bottom of this page, where $\overline{\delta}\left(x_S^{(D)}\left(t\right),\widetilde{x}_S^{(D)}\left(t\right)\right)=1$ if $x_S^{(D)}\left(t\right)\neq\widetilde{x}_S^{(D)}\left(t\right)$ and $\overline{\delta}\left(x_S^{(D)}\left(t\right),\widetilde{x}_S^{(D)}\left(t\right)\right)=0$ if $x_S^{(D)}\left(t\right)=\widetilde{x}_S^{(D)}\left(t\right)$.

Remark 2: As defined earlier, $\mathrm{ASEP}_{\mathrm{e}}^{(SRD)}$ is the ASEP at the destination given that the relay demodulated the data from the source incorrectly. In other words, $\mathrm{ASEP}_{\mathrm{e}}^{(SRD)}$ is the error probability due to error propagation when the relay forwards an erroneous signal to the destination. The closed-form formulation of this error probability is analytically difficult. However, it can be approximated by the worst case value, $\mathrm{ASEP}_{\mathrm{e}}^{(SRD)}\approx 1-(1/M)$ [67], [68]. This approximation has been validated with the aid of extensive Monte Carlo simulations in Section VI. The tightness of the curves in Section VI justifies the usefulness of the approximation.

Finally, the overall end-to-end ASEP, i.e., $\mathrm{ASEP}_{\mathrm{SM-FDR}}$ can be computed in closed-form by inserting (25) and (16) in (7).

C. Diversity Analysis

In this section, we analyze the achievable diversity order of the SM-FDR protocol. From (7), the asymptotic error-probability of SM-FDR can be formulated as follows:

$$\mathrm{ASEP}_{\mathrm{SM-FDR}}\approx\left(1-(1/M)\right)\mathrm{ASEP}^{(SR)}+\mathrm{ASEP}_{\mathrm{c}}^{(SRD)}\tag{26}$$

From (26), it follows that the diversity order of $\mathrm{ASEP}_{\mathrm{SM-FDR}}$ is linked to $\mathrm{ASEP}^{(SR)}$ and $\mathrm{ASEP}_{\mathrm{c}}^{(SRD)}$, which depend on $\mathrm{APEP}^{(SR)}\left(\cdot\right)$ and $\mathrm{APEP}_{\mathrm{c}}^{(SRD)}\left(\cdot\right)$, respectively. Since the achievable diversity order, $\mathcal{D}_{\mathrm{SM-FDR}}$, is determined by the APEP with the smallest decaying exponent, we have $\mathcal{D}_{\mathrm{SM-FDR}}=\min\left\{\mathcal{D}^{(SR)},\mathcal{D}^{(SRD)}\right\}$, where $\mathcal{D}^{(SR)}$ and $\mathcal{D}^{(SRD)}$ are the diversity orders contributed by $\mathrm{APEP}^{(SR)}\left(\cdot\right)$ and $\mathrm{APEP}_{\mathrm{c}}^{(SRD)}\left(\cdot\right)$, respectively.

From (15), an asymptotic expression for $\mathrm{APEP}^{(SR)}\left(x_S^{(R)}\left(t\right)\rightarrow\widetilde{x}_S^{(R)}\left(t\right)\right)$ can be formulated as follows:

$$\begin{aligned}&\mathrm{APEP}^{(SR)}\left(x_S^{(R)}\left(t\right)\rightarrow\widetilde{x}_S^{(R)}\left(t\right)\right)\\&\approx\frac{1}{\pi}\int_0^{\pi/2}\left(\frac{2E_S\sigma_{SR}^2\left|\Delta_S^{(R)}\left(t\right)\right|^2}{4\sin^2\left(\theta\right)\left(N_0+2E_R|x_R\left(t\right)|^2\sigma_{RR}^2\right)}\right)^{-(N_R-1)}d\theta\\&=\left(\frac{2^{-3+2N_R}\Gamma\left(-0.5+N_R\right)}{\sqrt{\pi}\Gamma\left(N_R\right)}\right)\\&\times\left(\frac{2\sigma_{SR}^2\left|\Delta_S^{(R)}\left(t\right)\right|^2\left(E_S/N_0\right)}{1+\tau^{1-\lambda}|x_R\left(t\right)|^2\left(E_S/N_0\right)^{1-\lambda}}\right)^{-(N_R-1)}\end{aligned}\tag{27}$$

where we let $E_R=\tau E_S$, with $\tau>0$.

From (27), we conclude that $\mathcal{D}^{(SR)}=\lambda\left(N_R-1\right)$. For instance, if the quality of SI cancellation is very high (e.g., $\lambda\approx 1$), then the full diversity of N_R-1 can be achieved for the source-to-relay transmission. On the other hand, for a poor SI cancellation quality (e.g., $\lambda\approx 0$), the achieved diversity order is zero.

Similarly, based on (20), the asymptotic expression for $\mathrm{APEP}_{\mathrm{c}}^{(SRD)}\left(\mathbf{x}_S^{(D)}\rightarrow\widetilde{\mathbf{x}}_S^{(D)}\right)$ can be formulated as follows:

$$\begin{aligned}&\mathrm{APEP}_{\mathrm{c}}^{(SRD)}\left(\mathbf{x}_S^{(D)}\rightarrow\widetilde{\mathbf{x}}_S^{(D)}\right)\\&\approx\frac{1}{\pi}\int_0^{\pi/2}\left(\frac{\left(\mathcal{K}_{SD}/4\right)}{\sin^2\left(\theta\right)}\right)^{-1}\left(\frac{\left(\mathcal{K}_{RD}/4\right)}{\sin^2\left(\theta\right)}\right)^{-1}\\&=\left(8/3\right)\tau\sigma_{SD}^2\sigma_{R_pD}^2\left(\left|\Delta_S^{(D)}\left(t\right)\right|^2+\left|\Delta_S^{(D)}\left(t+1\right)\right|^2\right)^{-1}\\&\times\left(\rho_R\left(t+1\right)\right)^{-1}\times\left(E_S/N_0\right)^{-2}\end{aligned}\tag{28}$$

which readily reveals that $\mathcal{D}^{(SRD)}=2$.

Based on the obtained values of $\mathcal{D}^{(SR)}$ and $\mathcal{D}^{(SRD)}$, we conclude that the achievable diversity order of SM-FDR is $\mathcal{D}_{\mathrm{SM-FDR}}=\min\left\{\lambda\left(N_R-1\right),2\right\}$.

IV. Condition for the Superiority of SM-FDR over SM-HDR

Let us recall that the constant λ captures the quality of SI cancellation. A low value of λ ($\lambda\approx 0$) implies a poor-quality SI cancellation process, whereas a high value of λ ($\lambda\approx 1$) implies a good-quality SI cancellation process. The value of λ is directly linked to the hardware cost and the separation of antennas at the relay node; it is an important performance

$$\mathrm{ASEP}_{\mathrm{c}}^{(SRD)}=\frac{1}{M^2}\sum_{x_S^{(D)}(t)\in\mathcal{A}_S}\sum_{\widetilde{x}_S^{(D)}(t)\in\mathcal{A}_S}\sum_{x_S^{(D)}(t+1)\in\mathcal{A}_S}\sum_{\widetilde{x}_S^{(D)}(t+1)\in\mathcal{A}_S}\overline{\delta}\left(x_S^{(D)}\left(t\right),\widetilde{x}_S^{(D)}\left(t\right)\right)\mathrm{APEP}_{\mathrm{c}}^{(SRD)}\left(\mathbf{x}_S^{(D)}\rightarrow\widetilde{\mathbf{x}}_S^{(D)}\right)\tag{25}$$

metric and is of particular importance in analyzing the suitability of the FD transmission. Furthermore, the simulation results in Fig. 6 of Section VI reveals that the achievable rate of SM-FDR is worse than SM-HDR for certain values of λ. Therefore, a fundamental question naturally arises: *For what range of values of λ is SM-FDR better than SM-HDR?* In this section, we provide an answer to this fundamental question. More specifically, in this section, we derive mathematical expressions for computing the value of λ which is required for SM-FDR to outperform SM-HDR in terms of achievable rate. To proceed further, we first analyze the instantaneous achievable rate of SM-FDR and SM-HDR.

A. Instantaneous achievable rate Analysis

In SM-FDR, the relay first demodulates the source's data before forwarding it to the destination using SM (it is a decode-and-forward scheme). Using Theorem 1 in [69] (see also [70, Section III-A]), the achievable rate of SM-FDR can be formulated as follows:

$$\mathcal{C}_{\mathrm{SM-FDR}} = \max_{f(X_1,X_2)} \min\{I(X_1;Y_2|X_2), I(X_1,X_2;Y_3)\} \tag{29}$$

where X_1 is the source message, X_2 is the relay message, Y_2 is the received symbol at the relay, and Y_3 is the received symbol at the destination. The value of this expression depends on the degree of correlation between the source message X_1 and the relay message X_2. Assuming independence of X_1 and X_2[2], this reduces to:

$$\mathcal{C}_{\mathrm{SM-FDR}} = \min\left\{\mathcal{C}^{(SR)}_{\mathrm{SM-FDR}}, \mathcal{C}^{(SRD)}_{\mathrm{SM-FDR}}\right\} \tag{30}$$

where

1) $C^{(SR)}_{\mathrm{SM-FDR}} = I(X_1;Y_2)$ is the achievable rate of the links from source to relay (to achieve this, we assume that the source transmits i.i.d. Gaussian-distributed symbols), and includes the effects of the SI which is modeled as additive white Gaussian noise. Note that in the current context, Y_2 is a vector of length N_R-1. Using Shannon's theorem, the achievable instantaneous achievable rate of the source to relay links can be formulated as follows:

$$\mathcal{C}^{(SR)}_{\mathrm{SM-FDR}} = \log_2\left(1 + \sum_{p=1}^{N_R} \Pr\{p = \mathrm{Active}\} \times \sum_{\substack{r=1 \\ r\neq p}}^{N_R} \frac{(E_S/N_0)\left|h_{SR_r}\right|^2}{(E_R/N_0)\left|h_{R_pR_r}\right|^2 + 1}\right) \tag{31}$$

where $\Pr\{p = \mathrm{Active}\} = 1/N_R$ represents the probability that p-th antenna is active at the relay.

Remark 3: Recall that during the t-th time-slot ($t \neq 0$), one of the relay antennas is chosen for activation based on the source's demodulated symbol at the relay (in accordance with the principle of SM). The remaining N_R-1 antennas are in the receive mode. The equiprobability of the source's transmitted symbols might result in changes in the antennas that are in the transmit/receive mode during each time-slot. This directly influences the instantaneous achievable rate of the source to relay links, and therefore, the expression in (31) considers all the possible activation scenarios at the relay. Furthermore, the degrading effect of the SI on $\mathcal{C}^{(SR)}_{\mathrm{SM-FDR}}$ can also be seen explicitly in (31).

2) $C^{(SRD)}_{\mathrm{SM-FDR}} = I(X_1, X_2; Y_3)$ is the mutual information between the simultaneous transmissions from source and relay and the destination received symbol. To evaluate this, we make use of the the approach of Section III in [71]; note that here $X_2 = (X_2^{(\mathrm{M})}, X_2^{(\mathrm{CH})})$ where $X_2^{(\mathrm{M})}$ represents the symbol radiated from the relay's chosen transmit antenna and $X_2^{(\mathrm{CH})}$ denotes the index of that transmit antenna. So $I(X_1, X_2; Y_3) = I(X_1, X_2^{(\mathrm{M})}; Y_3|X_2^{(\mathrm{CH})}) + I(X_2^{(\mathrm{CH})}; Y_3)$. Assuming that the relay also transmits i.i.d. Gaussian-distributed symbols, the first term is given by:

$$I(X_1, X_2^{(\mathrm{M})}; Y_3|X_2^{(\mathrm{CH})}) = \frac{1}{N_R}\sum_{p=1}^{N_R} \log_2\left(1 + \frac{E_R}{N_0}\left|h_{R_pD}\right|^2 + \frac{E_S}{N_0}|h_{SD}|^2\right) \tag{32}$$

and the second term is given by (see [71] for definition):

$$I(X_2^{(\mathrm{CH})}; Y_3) = \log_2\left(\chi^{(\mathcal{SM})}_{\mathrm{spatial}}(\mathbf{h}_{RD})\right) \tag{33}$$

and represents the achievable rate that is linked to the spatial constellation diagram in an SM transmission, with $\mathbf{h}_{RD}$ emphasizing that $\chi^{(\mathcal{SM})}_{\mathrm{spatial}}$ is a function of relay-to-destination channels. In summary:

$$\mathcal{C}^{(SRD)}_{\mathrm{SM-FDR}} = \frac{1}{N_R}\sum_{p=1}^{N_R} \log_2\left(1 + \frac{E_R}{N_0}\left|h_{R_pD}\right|^2 + \frac{E_S}{N_0}|h_{SD}|^2\right) + \log_2\left(\chi^{(\mathcal{SM})}_{\mathrm{spatial}}(\mathbf{h}_{RD})\right) \tag{34}$$

Finally, we note that our definition of achievable rate considers only the case where the relay *always* decodes and forwards its received data; this is because we are interested in capturing the gains in achievable rate which are specifically due to the existence of full-duplex SM relaying.

Recently, several researchers have investigated the achievable rate limits of SM for gaussian inputs [71]–[73]. Usually, the achievable rate of SM is expressed as the summation of the achievable rate achieved achieved by the signal constellation diagram and that achieved by the spatial constellation diagram. In general, $\chi^{(\mathcal{SM})}_{\mathrm{spatial}}$ is relatively harder to formulate owing to the particular operating principle of SM. Several attempts have been made in this regard with varying levels of accuracy and complexity. In particular, $\chi^{(\mathcal{SM})}_{\mathrm{spatial}}$ provided in [71] requires computationally intensive summation of integrals, but achieves a high level of accuracy. In [72], closed-form upper and lower

[2]Note that the assumption here is of independence between the information symbols underlying the codewords *concurrently* transmitted from source and relay.

bounds have been proposed using Jensen's inequality, and has relatively low computational complexity. These bounds, although they only describe the trends of the achievable rate, are useful for optimization of SM systems. A more accurate achievable rate analysis has been provided in [73] for SM systems with complex Gaussian, real Gaussian and constant modulus amplitude-phase modulation (APM) symbol distribution. The interested reader is referred to [73, Section I] and the references therein for further information.

The achievable rate expression of (34) is general, and any of the expressions provided in the above-mentioned literature may be used, and may serve for different purposes. Finally, by inserting (31) and (34) in (30), the achievable instantaneous achievable rate of SM-FDR can be computed. The ergodic achievable rate of SM-FDR can be obtained by taking the expectation with respect to channel fading in (30). The computation of this expectation in closed-form is quite cumbersome and so numerical methods need to be used. In this paper, the ergodic achievable rate is evaluated with the aid of Monte Carlo simulations, the results of which are provided in Section VI.

For the sake of comparison, we also provide below the achievable rate of the SM-HDR protocol. In SM-HDR, the transmission protocol consists of two non-overlapping time-slots. During the first time-slot, the source broadcasts its data to the destination and the relay, where all the N_R antennas are in the receive mode. During the next time-slot, the relay applies SM to forward the data it received during the previous time-slot. At the destination, the demodulator provided in Table I is used to jointly process the data received during both time-slots. It is worth emphasizing that, in SM-HDR, owing to its HD operation, there is no SI distorting the the reception at the relay. Accordingly, the instantaneous achievable achievable rate of SM-HDR can be formulated as follows:

$$\mathcal{C}_{\mathrm{SM-HDR}} = \frac{1}{2}\min\left\{\mathcal{C}^{(SR)}_{\mathrm{SM-HDR}}, \mathcal{C}^{(SRD)}_{\mathrm{SM-HDR}}\right\} \tag{35}$$

where $\mathcal{C}^{(SR)}_{\mathrm{SM-HDR}} = \log_2\left(1+\sum_{p=1}^{N_R}(E_S/N_0)\left|h_{SR_r}\right|^2\right)$, and $\mathcal{C}^{(SRD)}_{\mathrm{SM-HDR}} = \mathcal{C}^{(SRD)}_{\mathrm{SM-FDR}}$ and is given by (34).

B. Requirement on the value of λ

We start by first re-writing the achievable rate expressions of SM-FDR and SM-HDR in Section IV-A as follows:

$$\begin{cases} \mathcal{C}_{\mathrm{SM-FDR}} = \log_2\left(1+\min\left\{\mathcal{G}^{(SR)}_{\mathrm{SM-FDR}}, \mathcal{G}^{(SRD)}_{\mathrm{SM-FDR}}\right\}\right) \\ \mathcal{G}^{(SR)}_{\mathrm{SM-FDR}} = \dfrac{1}{N_R}\displaystyle\sum_{p=1}^{N_R}\sum_{\substack{r=1\\ r\neq p}}^{N_R}\dfrac{(E_S/N_0)\left|h_{SR_r}\right|^2}{(E_R/N_0)\left|h_{R_pR_r}\right|^2+1} \\ \mathcal{G}^{(SRD)}_{\mathrm{SM-FDR}} = \chi^{(\mathcal{SM})}_{\mathrm{spatial}} \\ \quad \times\left[\displaystyle\prod_{p=1}^{N_R}\left(1+\frac{E_R}{N_0}\left|h_{R_pD}\right|^2+\frac{E_S}{N_0}\left|h_{SD}\right|^2\right)\right]^{\frac{1}{N_R}}-1 \end{cases} \tag{36}$$

$$\begin{cases} \mathcal{C}_{\mathrm{SM-HDR}} \\ \quad = \log_2\left(1+\sqrt{1+\min\left\{\mathcal{G}^{(SR)}_{\mathrm{SM-HDR}}, \mathcal{G}^{(SRD)}_{\mathrm{SM-HDR}}\right\}}-1\right) \\ \mathcal{G}^{(SR)}_{\mathrm{SM-HDR}} = \displaystyle\sum_{p=1}^{N_R}(E_S/N_0)\left|h_{SR_r}\right|^2 \\ \mathcal{G}^{(SRD)}_{\mathrm{SM-HDR}} = \mathcal{G}^{(SRD)}_{\mathrm{SM-FDR}} \end{cases} \tag{37}$$

Let λ^* be the sufficient value of λ for $\mathcal{C}_{\mathrm{SM-FDR}}$ to outperform $\mathcal{C}_{\mathrm{SM-HDR}}$, i.e., $\mathcal{C}_{\mathrm{SM-FDR}} \geq \mathcal{C}_{\mathrm{SM-HDR}}$ if and only if $\lambda \geq \lambda^*$.

Proposition 1: SM-FDR is preferred over SM-HDR if:

$$\lambda \geq \lambda^* = 1 - \frac{\ln\left(-1+\frac{2(N_R-1)\overline{\gamma}_{SR}(1+K_{RR})}{\overline{\mathcal{T}}_{\mathrm{SM-HDR}}(2+K_{RR})}\right)}{\ln\left(E_R/N_0\right)} \tag{38}$$

where

$$\begin{aligned} \overline{\mathcal{T}}_{\mathrm{SM-HDR}} &= \mathbb{E}_{\mathbf{h}_{\mathcal{T}_{\mathrm{SM-HDR}}}}\left\{\mathcal{T}_{\mathrm{SM-HDR}}\right\} \\ &= \mathbb{E}_{\mathbf{h}_{\mathcal{T}_{\mathrm{SM-HDR}}}}\left\{\sqrt{1+\min\left\{\mathcal{G}^{(SR)}_{\mathrm{SM-HDR}}, \mathcal{G}^{(SRD)}_{\mathrm{SM-HDR}}\right\}}-1\right\} \end{aligned} \tag{39}$$

with $\mathbf{h}_{\mathcal{T}_{\mathrm{SM-HDR}}}$ being the short-hand used to denote all fading channels in the expression of $\mathcal{T}_{\mathrm{SM-HDR}}$.

Proof: See Appendix II.

Equation (39) deserves some comments. 1) The expression for $\overline{\mathcal{T}}_{\mathrm{SM-HDR}}$ cannot, to the best of the authors' knowledge, be computed in closed-form. However, it can obtained numerically with the aid of standard computing software, such as Matlab and Mathematica. 2) From observation of (37), (38) and (39), it can be seen that decreasing E_R eases the constraint on the quality of SI cancellation, λ^*. This has also been verified with the aid of simulations in Section VI. These results suggest that optimal allocation of power can be used to further enhance the performance of SM-FDR. This scenario is, however, beyond the scope of the present paper and this topic is postponed to future research. 3) The value of λ^* obtained from (38) can also be used to obtain the value of the average SI channel SNR, $\overline{\gamma}_{RR}$ for SM-FDR to outperform SM-HDR. In particular, with the aid of (2), $\overline{\gamma}_{RR} = (E_R/N_0)^{1-\lambda}\left[(2+K_{RR})/(2+2K_{RR})\right]$.

V. Relay Selection Policies

In this section, we attempt to enhance the performance of the SM-FDR protocol by applying the concept of relay selection. Relay selection is an efficient approach to enhance the achievable rate and/or minimize the error probability by exploiting spatial diversity of the relays. Relay Selection for conventional FD cooperative systems have been considered in [74], [75]. The strategies in these papers are not directly suitable in SM-FDR because of the particular SM encoding process at the relay. Therefore, in this section we develop three relay selection policies specifically designed for SM-FDR.

We consider a scenario where L relays in the network, each with N_R antennas and with FD capability, are willing to forward the data of the source. In such a scenario, based

on some pre-defined selection policy, the destination selects one "best" relay to be part of relaying. In what follows, we provide two relay-selection policies for SM-FDR.

A. Policy I

The max-min policy is the most commonly used relay selection strategy in HD relay networks. We extend this approach for the SM-FDR protocol in order to maximize its achievable rate. Based on the achievable rate expression in (36), the relay selection policy for the selection of the best relay, $R_{\rm sel}$, can be formulated as follows:

$$R_{\rm sel} = \underset{\overline{R}\in\left\{R^{(1)},R^{(2)},\ldots,R^{(L)}\right\}}{\arg\max} \min\left\{\mathcal{G}_{\rm SM-FDR}^{(S\overline{R})}, \mathcal{G}_{\rm SM-FDR}^{(S\overline{R}D)}\right\} \tag{40}$$

where $\mathcal{G}_{\rm SM-FDR}^{(S\overline{R})}$ and $\mathcal{G}_{\rm SM-FDR}^{(S\overline{R}D)}$ are defined in (36). The expression of $\chi_{\rm sp}^{(\mathcal{SM})}\left(\mathbf{h}_{\overline{R}D}\right)$ in (36) is obtained from [72, Eq. 24]. This expression of $\chi_{\rm sp}^{(\mathcal{SM})}(\cdot)$ provides the best trade-off between complexity and accuracy, and is the most suited for the relay selection process.

B. Policy II

From Section VI (Fig. 6), it can be seen that SM-HDR outperforms SM-FDR for certain range of SNR and λ. Motivated by this consideration, we investigate a dynamic hybrid relay selection scheme that not only selects the best relay based on the instantaneous channel conditions of the L available relays, but also opportunistically switches between SM-FDR and SM-HDR modes. Based on (36) and (37), the hybrid relay selection policy can be formulated as follows:

$$\begin{aligned} &R_{\rm sel} \\ &= \underset{\bar{R}\in\left\{R^{(1)},R^{(2)},\ldots,R^{(L)}\right\}}{\arg\max} \max\left\{C_{\rm SM-FDR}\left(\bar{R}\right), C_{\rm SM-HDR}\left(\bar{R}\right)\right\} \end{aligned} \tag{41}$$

From Section VI, it will be evident that policy II provides a better than policy I due to the joint mode/relay selection.

C. Policy III

In Policy II, the relay selection is based on choosing the relay that provides the lowest (instantaneous) SEP at the destination. Accordingly, the relay selection policy can be formulated as follows:

$$R_{\rm sel} = \underset{\overline{R}\in\left\{R^{(1)},R^{(2)},\ldots,R^{(L)}\right\}}{\arg\min} \left\{\mathrm{SEP}_{\rm SM-FDR}\left(\bar{R}\right)\right\} \tag{42}$$

It is also worth noting that the direct link does not affect Policy III relay selection process, and hence, we need not take it into account in the utility function. Accordingly, $\mathrm{SEP}_{\rm SM-FDR}$ can be formulated as follows [59]:

$$\begin{aligned} &\mathrm{SEP}_{\rm SM-FDR}\left(\bar{R}\right) \\ &\quad\approx \mathrm{SEP}^{(S\overline{R})} + \mathrm{SEP}^{(\overline{R}D)} - 2\mathrm{SEP}^{(S\overline{R})}\mathrm{SEP}^{(\overline{R}D)} \\ &\overset{(\rm High-SNR)}{\approx} \mathrm{SEP}^{(S\overline{R})} + \mathrm{SEP}^{(\overline{R}D)} \end{aligned} \tag{43}$$

where $\mathrm{SEP}^{(S\overline{R})}$ and $\mathrm{SEP}^{(\overline{R}D)}$ are the instantaneous SEPs of the source-to-relay and relay-to-destination links. For the sake of illustration, in the following we assume that the SI channels are Rayleigh, and that PSK modulation is used at the source and the relay. From (15), (16) and (19), and with the aid of the NN approximation, they can be formulated as follows:

$$\begin{aligned} \mathrm{SEP}^{(S\overline{R})} &\approx N_{\Delta_{\min}}^{(S\overline{R})} Q\left(\sqrt{\sum_{p=1}^{N_R}\sum_{\substack{r=1\\r\neq p}}^{N_R} \frac{E_S\left|h_{S\overline{R}_r}\right|^2\left|\Delta_{\min}^{(S\overline{R})}\right|^2}{2\left(N_0+2E_R\sigma_{RR}^2\right)}}\right) \\ \mathrm{SEP}^{(\overline{R}D)} &\approx N_{\Delta_{\min}^{(\overline{R}D)}} Q\left(\sqrt{\frac{E_R\left|\Delta_{\min}^{(\overline{R}D)}\right|^2}{2N_0}}\right) \end{aligned} \tag{44}$$

where: i) $N_{\Delta_{\min}}^{(S\overline{R})}$ and $\Delta_{\min}^{(S\overline{R})}$ are defined in Section III-A; ii) $N_{\Delta_{\min}}^{(\overline{R}D)}$ is the number of signal- and spatial constellation diagrams with Euclidean distance $\left|\Delta_{\min}^{(\overline{R}D)}\right|$, with $\left|\Delta_{\min}^{(\overline{R}D)}\right|$ being the minimum Euclidean distance among all possible pairs of SM constellation points, which include both signal- and spatial constellation diagrams [63].

Based on (21), $\left|\Delta_{\min}^{(\overline{R}D)}\right|$ can be formulated as follows:

$$\begin{aligned} &\left|\Delta_{\min}^{(\overline{R}D)}\right| \\ &= \min_{\substack{p,\widetilde{p}\in\{1,2,..,N_R\};p\neq\widetilde{p}\\ x_{\overline{R}}^{(D)}(t+1),\widetilde{x}_{\overline{R}}^{(D)}(t+1)\in\mathcal{A}_R;\\ x_{\overline{R}}^{(D)}(t+1)\neq\widetilde{x}_{\overline{R}}^{(D)}(t+1)}} \left\{\left|h_{\overline{R}_pD}x_{\overline{R}}^{(D)}(t+1) - h_{\overline{R}_{\widetilde{p}}D}\widetilde{x}_{\overline{R}}^{(D)}(t+1)\right|\right\} \\ &= \min\left\{\left|\Delta_{\min}^{(\overline{R}D,1)}\right|, \left|\Delta_{\min}^{(\overline{R}D,2)}\right|, \left|\Delta_{\min}^{(\overline{R}D,3)}\right|\right\} \end{aligned} \tag{45}$$

where:

$$\begin{cases} \left|\Delta_{\min}^{(\overline{R}D,1)}\right|^2 = \min\limits_{p\in\{1,2,..,N_R\}}\left\{\left|h_{\overline{R}_pD}\right|^2\right\} \\ \quad\times \min\limits_{\substack{x_{\overline{R}}^{(D)}(t+1),\widetilde{x}_{\overline{R}}^{(D)}(t+1)\in\mathcal{A}_R;\\ x_{\overline{R}}^{(D)}(t+1)\neq\widetilde{x}_{\overline{R}}^{(D)}(t+1)}}\left\{\left|x_{\overline{R}}^{(D)}(t+1) - \widetilde{x}_{\overline{R}}^{(D)}(t+1)\right|^2\right\} \\ \qquad = \min\limits_{p\in\{1,2,..,N_R\}}\left\{\left|h_{\overline{R}_pD}\right|^2\right\} 4\sin^2\left(\frac{\pi}{M}\right); \\ \qquad \text{if} \quad p=\widetilde{p} \quad \text{and} \quad x_{\overline{R}}^{(D)}(t+1)\neq\widetilde{x}_{\overline{R}}^{(D)}(t+1) \end{cases} \tag{46}$$

$$\left\{\begin{array}{l}\left|\Delta_{\min}^{(\overline{R}D,2)}\right|^2 = \min\limits_{p,\widetilde{p}\in\{1,2,..,N_R\};p\neq\widetilde{p}}\left\{\left|h_{\overline{R}_pD}-h_{\overline{R}_{\widetilde{p}}D}\right|^2\right\} \\ \qquad\qquad \times \min\limits_{x_{\overline{R}}^{(D)}(t+1)\in\mathcal{A}_R}\left\{\left|x_{\overline{R}}^{(D)}(t+1)\right|^2\right\} \\ \qquad\qquad = \min\limits_{p,\widetilde{p}\in\{1,2,..,N_R\};p\neq\widetilde{p}}\left\{\left|h_{\overline{R}_pD}-h_{\overline{R}_{\widetilde{p}}D}\right|^2\right\}; \\ \qquad\qquad \text{if} \quad p\neq\widetilde{p} \quad \text{and} \quad x_{\overline{R}}^{(D)}(t+1)=\widetilde{x}_{\overline{R}}^{(D)}(t+1)\end{array}\right. \tag{47}$$

$$\left\{\begin{array}{l}\left|\Delta_{\min}^{(\overline{R}D,3)}\right|^2 \\ = \min\limits_{\substack{p,\widetilde{p}\in\{1,2,..,N_R\};\\ p\neq\widetilde{p}}} \mathbb{E}_{\substack{x_{\overline{R}}^{(D)}(t+1),\\ \widetilde{x}_{\overline{R}}^{(D)}(t+1)}}\left\{\left|h_{\overline{R}_pD}x_{\overline{R}}^{(D)}(t+1)\right.\right. \\ \qquad\qquad \left.\left.-h_{\overline{R}_{\widetilde{p}}D}\widetilde{x}_{\overline{R}}^{(D)}(t+1)\right|^2\right\} \\ \overset{(a)}{=} \min\limits_{p,\widetilde{p}\in\{1,2,..,N_R\};p\neq p'}\frac{1}{M^2}\times\sum\limits_{x_{\overline{R}}^{(D)}(t+1)\in\mathcal{A}_R} \\ \sum\limits_{\widetilde{x}_{\overline{R}}^{(D)}(t+1)\in\mathcal{A}_R}\left|h_{\overline{R}_pD}x_{\overline{R}}^{(D)}(t+1)-h_{\overline{R}_{\widetilde{p}}D}\widetilde{x}_{\overline{R}}^{(D)}(t+1)\right|^2; \\ \qquad\qquad \text{if} \quad p\neq\widetilde{p} \quad \text{and} \quad x_{\overline{R}}^{(D)}(t+1)\neq\widetilde{x}_{\overline{R}}^{(D)}(t+1)\end{array}\right. \tag{48}$$

where (a) follows by averaging out the symbols in order to make the relay selection policy independent of the transmitted symbols.

The final expression for $\mathrm{SEP}^{(\overline{R}D)}$ can be obtained by substituting (45)-(48) in (44). Having obtained $\mathrm{SEP}^{(S\overline{R})}$ and $\mathrm{SEP}^{(\overline{R}D)}$, the best relay can be selected using the criterion in (42).

Remark 4: The relay selection strategies of Policy I and Policy II requires the estimation of instantaneous SI channels at the relay, which should then be forwarded to the destination or a centralized controller. The relay can either exploit channel estimation techniques already available for HD systems, or it can rely on techniques specifically tailored to estimate SI channels. However, the perfect estimation of SI channels are difficult to realize in practice due to the reasons outlined in [18]. On the other hand, Policy III requires the knowledge of only the variance, $\sigma^2_{\overline{R}_p\overline{R}_r}$ of the SI channels. This significantly reduces the overhead of the relay selection process.

VI. Numerical and Simulation Results

In this section, we present numerical results in order to assess the performance of SM-FDR, to verify the accuracy of the proposed mathematical framework, to substantiate our claims made in Section IV and Section V, as well as to compare the performance against traditional FD relaying.

a) Simulation setup: The system model introduced in Section II-A is accurately reproduced in our simulation environment. For the ease of illustration, the results are obtained under the following general assumptions: i) i.i.d. fading with $\sigma^2_{SR_r}=\sigma^2_{R_rD}=\sigma^2_{SD}=1/2$, for $r=1,2,...,N_R$; ii) the Rician factor $K_{R_pR_r}=K_{RR}$, for $r,p\in\{1,2,...,N_R\}$, with $r\neq p$; iii) unless explicitly specified, the source and the relay transmit with the same average energy, i.e., $E_S=E_R=E_M$. Furthermore, for the sake of a fair comparison, E_M for all the considered relaying protocols is assumed to be the same; and iv) also for a fair comparison, the average rate in bits per channel use (bpcu) for the relaying protocols is considered to be the same. For instance, for a given M, the average rate of SM-FDR is $\log_2(M)$ bpcu, whereas that of SM-HDR is $1/2\,(\log_2(M))$ bpcu. Therefore, for instance, if $M=4$ is used for SM-FDR, then $M=16$ is considered for SM-HDR. Other simulation parameters are provided in the caption of the figures.

b) Impact of direct connectivity and comparison with SM-HDR and single–hop transmission: In Fig. 2 and Fig. 3, the end-to-end ASEP of SM-FDR employing the demodulator developed in Section II–D is compared against "SM-FDR-

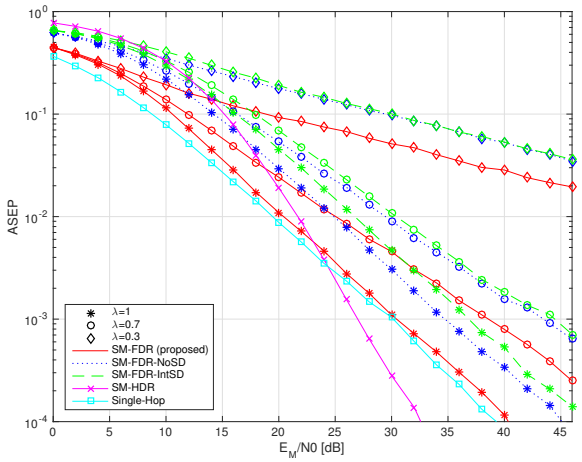

Fig. 2: ASEP of different demodulators for SM-FDR (as summarized in Table I) and comparison with SM-HDR. Setup: $M=4$ (PSK), $N_R=2$, $K_{RR}=1$ and $\lambda=\{1,0.7,0.3\}$ for SM-FDR; $M=16$ (PSK) and $N_R=2$ for SM-HDR; and $M=4$ (PSK) for single–hop transmission.

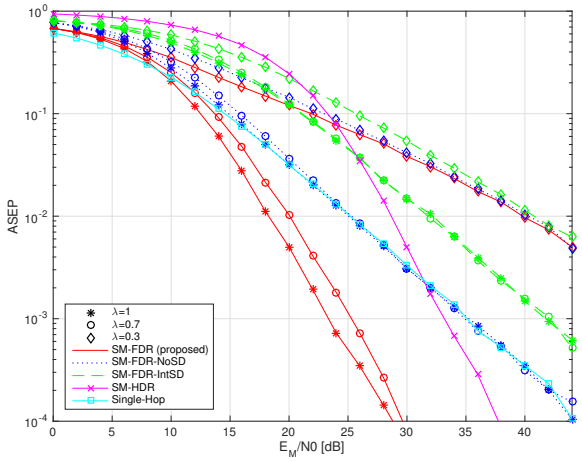

Fig. 3: ASEP of different demodulators for SM-FDR (as summarized in Table I) and comparison with SM-HDR. Setup: $M=8$ (PSK), $N_R=4$, $K_{RR}=1$ and $\lambda=\{1,0.7,0.3\}$ for SM-FDR; $M=64$ (PSK) and $N_R=4$ for SM-HDR; and $M=8$ (PSK) for single–hop transmission.

TABLE I: Summary of demodulators for the protocols analyzed in Section VI. Notation: i) $\left(p, x_R^{(D)}(t)\right) = \mathcal{SM}\left(\mathcal{B}\left(\widehat{x}_S^{(D)}(t-1)\right)\right)$; ii) $\left(\widetilde{p'}, \widetilde{x}_R^{(D)}(t+1)\right) = \mathcal{SM}\left(\mathcal{B}\left(\widetilde{x}_S^{(D)}(t)\right)\right)$; and iii) $G_{\mathrm{AF}} = \frac{1}{\sqrt{E_S|h_{SR}|^2 + E_R|h_{RR}|^2 N_0}}$.

SM-FDR
$\widehat{x}_S^{(D)}(t) = \underset{\substack{\widetilde{x}_S^{(D)}(t)\in\mathcal{A}_S \\ \widetilde{x}_S^{(D)}(t+1)\in\mathcal{A}_S}}{\arg\min} \left\{\Lambda^{(D)}\left(\widetilde{x}_S^{(D)}(t), \widetilde{x}_S^{(D)}(t+1)\right)\right\}$
$\Lambda^{(D)}\left(\widetilde{x}_S^{(D)}(t), \widetilde{x}_S^{(D)}(t+1)\right) = \left\|y_D(t) - \left(\sqrt{E_S}h_{SD}\widetilde{x}_S^{(D)}(t) + \sqrt{E_R}h_{R_pD}x_R^{(D)}(t)\right)\right\|^2 + \left\|y_D(t+1) - \left(\sqrt{E_S}h_{SD}\widetilde{x}_S^{(D)}(t+1) + \sqrt{E_R}h_{R_{\widetilde{p'}}D}\widetilde{x}_R^{(D)}(t+1)\right)\right\|^2$
SM-FDR-NoSD
$\hat{x}_S^{(D)}(t+1) = \underset{\widetilde{x}_S^{(D)}(t)\in\mathcal{A}_S}{\arg\min} \left\{\Lambda^{(D)}\left(\widetilde{x}_S^{(D)}(t)\right)\right\}$
$\Lambda^{(D)}\left(\widetilde{x}_S^{(D)}(t)\right) = \left\|y_D(t+1) - \left(\sqrt{E_R}h_{R_{\widetilde{p'}}D}\widetilde{x}_R^{(D)}(t+1)\right)\right\|^2$
SM-FDR-IntSD
$\widehat{x}_S^{(D)}(t) = \underset{\substack{\widetilde{x}_S^{(D)}(t)\in\mathcal{A}_S \\ \widetilde{x}_S^{(D)}(t+1)\in\mathcal{A}_S}}{\arg\min} \left\{\Lambda^{(D)}\left(\widetilde{x}_S^{(D)}(t)\right)\right\}$
$\Lambda^{(D)}\left(\widetilde{x}_S^{(D)}(t)\right) = \left\|y_D(t+1) - \left(\sqrt{E_S}h_{SD}\widetilde{x}_S^{(D)}(t+1) + \sqrt{E_R}h_{R_{\widetilde{p'}}D}\widetilde{x}_R^{(D)}(t+1)\right)\right\|^2$
DF-FDR
$\widehat{x}_S^{(D)}(t) = \underset{\substack{\widetilde{x}_S^{(D)}(t)\in\mathcal{A}_S \\ \widetilde{x}_S^{(D)}(t+1)\in\mathcal{A}_S}}{\arg\min} \left\{\Lambda^{(D)}\left(\widetilde{x}_S^{(D)}(t), \widetilde{x}_S^{(D)}(t+1)\right)\right\}$
$\Lambda^{(D)}\left(\widetilde{x}_S^{(D)}(t), \widetilde{x}_S^{(D)}(t+1)\right) = \left\|y_D(t) - \left(\sqrt{E_S}h_{SD}\widetilde{x}_S^{(D)}(t) + \sqrt{E_R}h_{RD}\hat{x}_S^{(D)}(t-1)\right)\right\|^2 + \left\|y_D(t+1) - \left(\sqrt{E_S}h_{SD}\widetilde{x}_S^{(D)}(t+1) + \sqrt{E_R}h_{RD}\widetilde{x}_S^{(D)}(t)\right)\right\|^2$
AF-FDR
$\widehat{x}_S^{(D)}(t) = \underset{\substack{\widetilde{x}_S^{(D)}(t)\in\mathcal{A}_S \\ \widetilde{x}_S^{(D)}(t+1)\in\mathcal{A}_S}}{\arg\min} \left\{\Lambda^{(D)}\left(\widetilde{x}_S^{(D)}(t), \widetilde{x}_S^{(D)}(t+1)\right)\right\}$
$\Lambda^{(D)}\left(\widetilde{x}_S^{(D)}(t), \widetilde{x}_S^{(D)}(t+1)\right) = \left\|y_D(t) - \left(\sqrt{E_S}h_{SD}\widetilde{x}_S^{(D)}(t) + \sqrt{E_R}h_{RD}\left(G_{\mathrm{AF}}\sqrt{E_S}h_{SR}\hat{x}_S^{(D)}(t-1)\right)\right)\right\|^2 + \left\|y_D(t+1) - \left(\sqrt{E_S}h_{SD}\widetilde{x}_S^{(D)}(t+1) + \sqrt{E_R}h_{RD}\left(G_{\mathrm{AF}}\sqrt{E_S}h_{SR}\widetilde{x}_S^{(D)}(t)\right)\right)\right\|^2$
HD-FDR
$\hat{x}_S^{(D)}(t) = \underset{\widetilde{x}_S^{(D)}(t)\in\mathcal{A}_S}{\arg\min} \left\{\Lambda^{(D)}\left(\widetilde{x}_S^{(D)}(t)\right)\right\}$
$\Lambda^{(D)}\left(\widetilde{x}_S^{(D)}(t), \widetilde{x}_S^{(D)}(t+1)\right) = \left\|y_D(t) - \left(\sqrt{E_S}h_{SD}\widetilde{x}_S^{(D)}(t)\right)\right\|^2 + \left\|y_D(t+1) - \left(\sqrt{E_R}h_{R_{\widetilde{p'}}D}\widetilde{x}_R^{(D)}(t+1)\right)\right\|^2$

NoSD" and "SM-FDR-IntSD". More specifically, SM-FDR-NoSD refers to the SM-FDR protocol where a direct link from the source is not available at the destination, and SM-FDR-IntSD refers to the SM-FDR protocol where the direct link is treated as interference, but exploits its full knowledge. The corresponding demodulators are summarized in Table I. The results clearly show that the demodulator in Section II–D provides a significant improvement in the ASEP performance over SM-FDR-NoSD and SM-FDR-IntSD, which confirms the benefit of exploiting the direct connectivity in FD relaying.

In Fig. 2 and Fig. 3, SM-FDR is also compared against SM-HDR and single-hop transmission (i.e., the protocol where the source communicates directly with the destination without using a relay node). In particular, we observe that: i) if $N_R = 2$, SM-FDR outperforms SM-HDR for low SNR values, whereas for high SNR values, SM-HDR has a clear advantage. On the other hand, when compared against single-hop transmission, SM-FDR has a slightly lower performance when $N_R = 2$; and ii) if $N_R = 4$, SM-FDR, with relatively higher values of λ, is significantly better than SM-HDR and single-hop transmission. The reason behind these trends is as follows. When $N_R = 2$, the number of antennas available for reception at the relay is two for SM-HDR, and only one for SM-FDR. This leads to increased reception quality in the

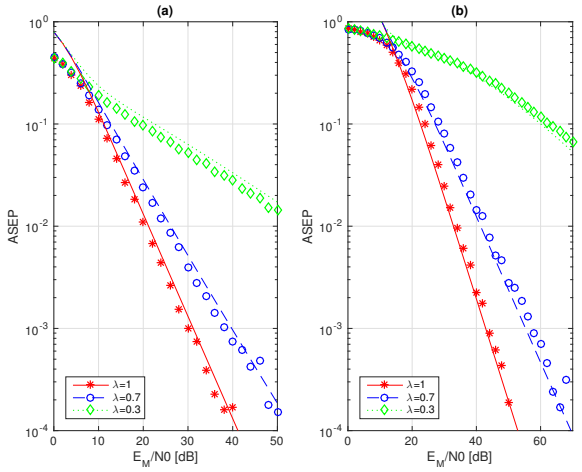

Fig. 4: Comparison of Monte Carlo simulations (markers) and the mathematical framework (solid/dashed/dotted lines) in (7), (14), (16) and (25). Setup: (a) $M = 4$ (PSK), $N_R = 2$ and $K_{RR} = 1$. (b) $M = 16$ (QAM), $N_R = 2$ and $K_{RR} = 5$.

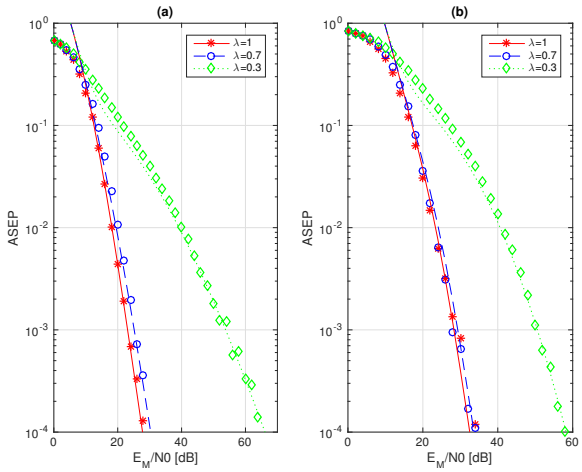

Fig. 5: Comparison of Monte Carlo simulations (markers) and the mathematical framework (solid/dashed/dotted lines) in (7), (15), (16) and (25). Setup: (a) $M = 8$ (PSK), $N_R = 4$ and $K_{RR} = 0$. (b) $M = 16$ (PSK), $N_R = 8$ and $K_{RR} = 0$.

source-relay transmission for SM-HDR, which translates to its overall better error-performance in the high SNR regime. In the case of single-hop transmission, for a fair comparison, we considered that the source transmits with energy[3] $E_S = 2E_M$. This energy consideration benefits single-hop transmission and leads to its better performance when $N_R = 2$. When $N_R = 4$, however, the smaller constellation size used in SM-FDR, originating from the use of reduced number of channel-uses/time-slots, has a stronger impact. This leads to the superiority of SM-FDR over SM-HDR. Furthermore, the diversity gain originating from larger N_R makes SM-FDR perform significantly better than single-hop transmission. Note that the achievable diversity order of SM-FDR is $\min\{\lambda(N_R - 1), 2\}$ (see Section III–C) and that of single-hop transmission is always one. Although not shown here due to space limitations,

[3]Note that the total energy consumed in SM-FDR and SM-HDR to forward an information symbol to the destination is $E_S + E_R = 2E_M$.

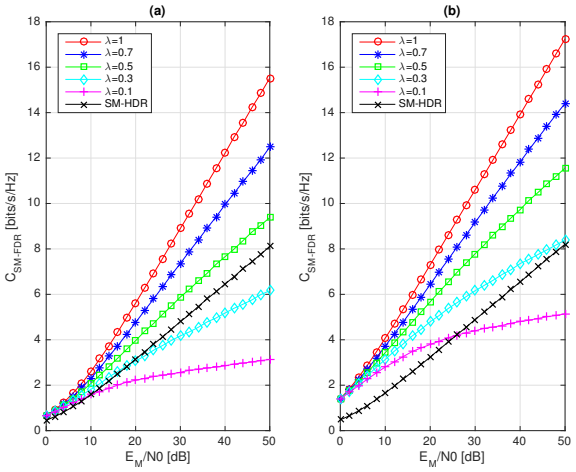

Fig. 6: Simulation results for achievable rate of SM-FDR for various values of λ_R, and comparison with SM-HDR. Setup: (a) $N_R = 2$ and $K_{RR} = 1$. (b) $N_R = 4$ and $K_{RR} = 1$.

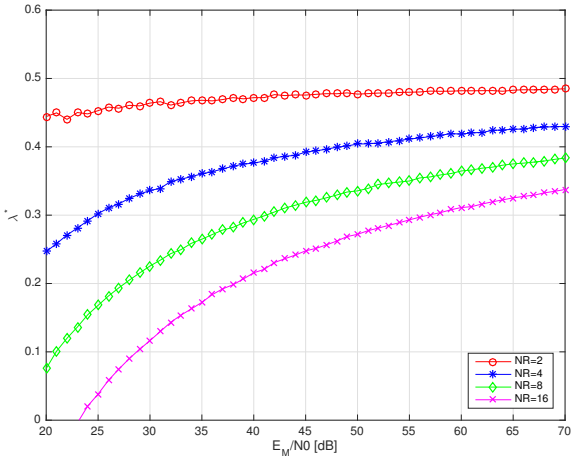

Fig. 7: The value of λ^* obtained using (38) for various N_R. Setup: $K_{RR} = 1$.

trends similar to $N_R = 4$ also holds for $N_R > 4$. Overall, these results confirm the potential of SM-FDR for achieving high throughput

c) Validation of the mathematical framework: In Figs. 4 and 5, the accuracy of the proposed mathematical framework is investigated by comparing it against Monte Carlo simulations for various system setups. The results confirm the high accuracy of the mathematical framework and validate the approximations proposed in Section III-A and Section III-B. Indeed, as expected, the ASEP degrades as λ decreases. More importantly, the numerical examples also confirm our findings about the achievable diversity order of SM-FDR, which has been provided as a function of λ and N_R in Section III-C.

d) Analysis of the achievable rate: In Fig. 6, the achievable rate of SM-FDR for various system setups is analyzed. As expected, the results clearly show that achievable rate increases with increasing λ. Furthermore, comparison of Fig. 6.a and Fig. 6.b reveals that the achievable rate increases with increasing N_R. The reason is that the robustness of the source-

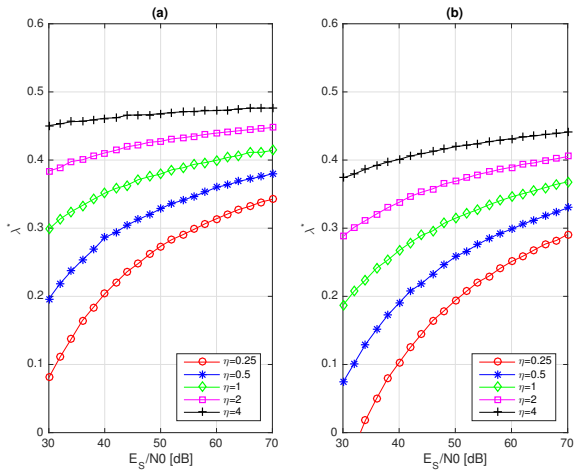

Fig. 8: The value of λ^* obtained using (38) for various η where $\eta = E_R/E_S$. Setup: (a) $N_R = 4$ and $K_{RR} = 5$. (b) $N_R = 8$ and $K_{RR} = 5$.

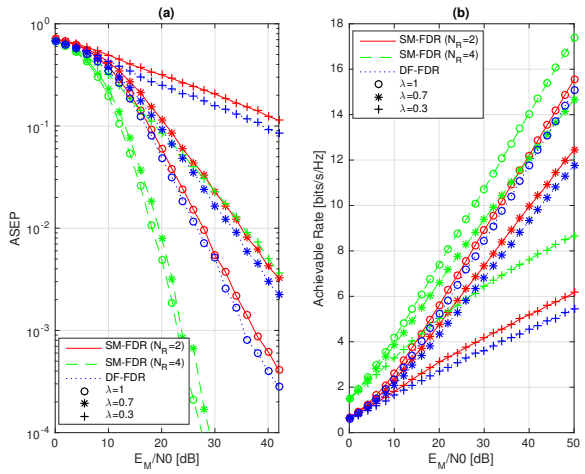

Fig. 10: Performance comparison of SM-FDR against DF-FDR. Setup: (a) $M = 8$ (PSK) and $K_{RR} = 1$. (b) $K_{RR} = 1$.

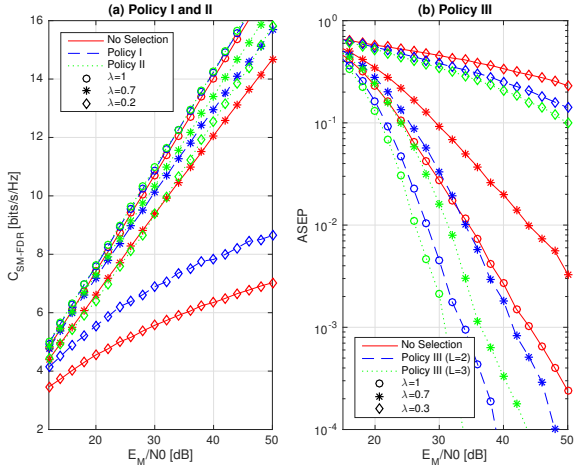

Fig. 9: Performance comparison of SM-FDR with and without relay selection. Setup: (a) *Policy I* and *Policy II:* $N_R = 4$, $K_{RR} = 1$, and $L = 4$. (b) *Policy III:* $N_R = 2$ and $K_{RR} = 1$.

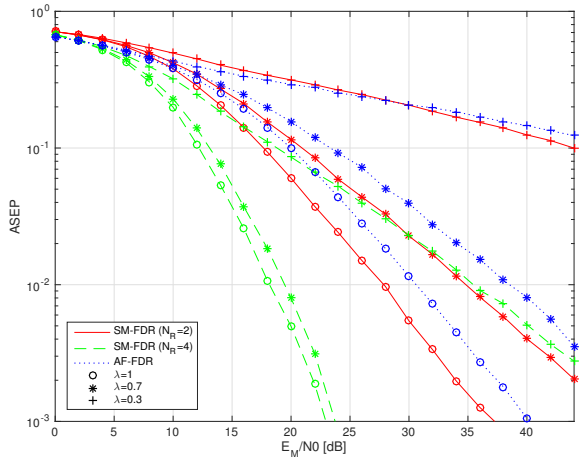

Fig. 11: ASEP comparison of SM-FDR against AF-FDR. Setup: $M = 8$ (PSK) and $K_{RR} = 1$.

to-relay transmission increases as N_R increases. For the sake of comparison, in Fig. 6 we also show the achievable rate of SM-HDR. In general, the results show that SM-HDR achieves a higher achievable rate compared to SM-FDR for smaller values of λ. More specifically, in the high-SNR regime, SM-HDR is better than SM-FDR for $\lambda < 0.5$ if $N_R = 2$, and for $\lambda < 0.3$ if $N_R = 4$. These trends confirm the need of the analytical development provided in Section IV, where mathematical expressions for computing the range of λ for which SM-FDR is suitable over SM-HDR has been provided.

e) Evaluation of the SI cancellation quality requirement: In Fig. 7 and Fig. 8, we evaluate λ^*, i.e., sufficient value of λ for which SM-FDR has a better performance than SM-HDR, under various system parameters. We observe that the value of λ^* is, in general, less than 0.5. Furthermore, we also observe that λ^* decreases with increasing N_R. This is expected as increasing N_R also increases the relay's reception quality. In addition, Fig. 8 reveals that the constraint on λ^* can be eased by decreasing E_R. However, it should be noted that decreasing E_R will also adversely effect the relay-to-destination signal quality, and hence the overall error performance and the achievable rate. These trends indicate the need for the optimization of relay's transmit energy. Transmit energy optimization in SM-FDR, although not considered in this paper due to space limitations, is an interesting future line of research. We believe that the optimization methodology used in [76] for conventional FD relaying can be adapted for use in SM-FDR. Finally, as previously remarked in Section IV, the obtained λ^* value can also be used to compute the sufficient value of $\overline{\gamma}_{RR}$ (in dB) for SM-FDR to outperform SM-HDR.

f) Performance enhancement with relay selection: In Fig. 9, we investigate the potential gain of combining SM-FDR with the proposed relay selection policies, namely Policy I, Policy II and Policy III. We analyze the scenarios where there are L FD relays available in the network to forward the source's data. With the aid of the relay selection policies

presented in Section V, one best relay is chosen out of the L available relays. The results confirm the usefulness of the proposed relay selection policies for performance enhancement. In particular, Fig. 9.a shows that achievable rate gain can be achieved using Policy I and Policy II. Furthermore, Policy II, i.e., hybrid relay selection policy performs significantly better than Policy I. This is because Policy II jointly selects both the best mode (SM-FDR/SM-HDR), as well as the best relay. Fig. 9.b shows that a significant coding and/or diversity gain can be achieved using Policy II. Furthermore, the gain increases with increasing L.

g) Performance comparison with traditional FD relaying protocols: In Fig. 10 and Fig. 11, a performance comparison of the SM-FDR protocol against traditional FD relaying protocols is provided. More specifically, we compare SM-FDR against DF-based FD relaying (referred to as DF-FDR) and AF-based FD relaying (referred to as AF-FDR) [26]. In both DF-FDR and AF-FDR, a single fixed transmit and receive antenna of the relay is used for the FD relaying process. Note that all the three protocols under consideration have the same number of active RF chains, which contribute to most of the energy consumption at the relay. Furthermore, using arguments similar to Section II-D, a demodulator similar to (6) has been developed and used in these cases also (see Table I). Accordingly, the performance comparison among the protocols is fair in terms of total transmit energy consumption, as well as demodulation complexity. The following general conclusions can be drawn. 1) If $N_R = 2$, the ASEP of DF-FDR is slightly better than SM-FDR. This result follows the same trend as that of Single-Input-Singe-Output (SISO) and conventional point-to-point SM systems with only one receive antenna [33]. 2) If $N_R = 4$, the ASEP of SM-FDR is always better than DF-FDR. The price to be paid, however, is the need for larger antenna array (with only one of them active) at the relay, which results in increased reception quality for the source-to-relay transmission. 3) The achievable rate of SM-FDR for both $N_R = 2$ and $N_R = 4$ is better than DF-FDR, thanks to the additional degree of freedom in the form of the spatial constellation diagram offered by SM. 4) SM-FDR, for both $N_R = 2$ and $N_R = 4$, is superior to AF-FDR in terms of ASEP. Although not shown here for brevity, the performance trends for $N_R > 4$ are similar to $N_R = 4$. We may therefore conclude that SM-FDR has a slight advantage in terms of achievable rate, and the DF-FDR has a slight advantage from the perspective of the ASEP.

VII. Conclusion

In this paper, we have analyzed the performance of SM-FDR, which is a new FD relaying protocol based on the concept of single-RF SM. A mathematical frameworks for the analysis of SM-FDR in the presence of SI channels has been developed, and has been substantiated with the aid of Monte Carlo simulations. The analysis has revealed important insights on the performance that may emerge, depending on the SNR operating regime, the fading parameters, the number of antennas available at the relay and the quality of SI cancellation. Thereafter, we derived mathematical expressions for computing the achievable rate of SM-FDR. Based on these expressions, we introduced a model that can accurately predict the quality of SI cancellation required for SM-FDR to outperform SM-HDR. Finally, we developed three relay selection policies specifically designed for the SM-FDR protocol. The results revealed the potential gain of combining SM-FDR with relay selection, both in terms of achievable rate and error performance.

The recent white paper on research beyond 5G released by the NetWorld2020 European Technology platform, a member of the Fifth Generation Infrastructure Public Private Partnership (5G PPP) association, has emphasized the importance of SM for the practical realization of massive MIMO [77]. This inference can be mainly attributed to the energy-efficiency advantage of SM owing to its single-RF property. Based on this consideration, a key direction for future research is to develop a FD relaying protocol, which judiciously combines SM-FDR with a massive MIMO relay. A appropriate transmit beamforming and transmit power optimization techniques need to be developed, and these are currently under investigation by the authors.

Appendix I
Derivation of $\mathrm{APEP}_{\mathrm{NI}}^{(SR)}\left(x_S^{(R)}(t) \to \widetilde{x}_S^{(R)}(t)\right)$

From (11) and (12), $\mathrm{APEP}_{\mathrm{NI}}^{(SR)}\left(x_S^{(R)}(t) \to \widetilde{x}_S^{(R)}(t)\right)$ can be formulated as in (49), shown at the bottom of this page.

First, we compute the CF of $\overline{n}_R$, $\Phi_{\overline{n}_R}(\cdot)$, as follows:

$$\Phi_{\overline{n}_R}(\omega) = \mathbb{E}_{\overline{n}_R}\left\{\exp\left(j\omega\overline{n}_R\right)\right\} \overset{(a)}{=} \exp\left(-(1/4)\,N_0\omega^2\right) \quad (50)$$

where (a) follows by noting that $\overline{n}_R$ is a Gaussian RV and with the aid of [64, Eq. (5)].

Then, we compute the CF of $\overline{I}_R$, $\Phi_{\overline{I}_R}(\cdot)$, as follows:

$$\begin{aligned}\Phi_{\overline{I}_R}(\omega) &= \mathbb{E}_{\theta_{h_{SR}},\bar{h}_{RR}}\Big\{\exp\Big(j\omega\sqrt{E_R}\,|x_R(t)|\left(\mathrm{Re}\left\{\bar{h}_{RR}\right\}\right.\\ &\qquad\left.+\mu_{RR}\cos\left(\theta_{h_{SR}}+\bar{\theta}_R\right)\right)\Big)\Big\}\\ &\overset{(a)}{=}\frac{1}{2\pi}\int_0^{2\pi}\exp\left(j\omega\sqrt{E_R}\,|x_R(t)|\,\mu_{RR}\cos\left(\theta_{h_{SR}}+\overline{\theta}_R\right)\right)\\ &\qquad\times\exp\left(-(1/4)\,E_R|x_R(t)|^2\sigma_{RR}^2\omega^2\right)d\theta_{h_{SR}}\\ &=\exp\left(-(1/4)\,E_R|x_R(t)|^2\sigma_{RR}^2\omega^2\right)\\ &\times\mathrm{J}_0\left(\sqrt{E_R}\,|x_R(t)|\,\mu_{RR}\omega\right)\end{aligned} \quad (51)$$

where: i) (a) follows from [64, Eq. (5)] and by noting that $\theta_{h_{SR}}$ is a uniformly distributed RV. Also note that adding a constant phase term, $\overline{\theta}_R$ to a uniformly distributed phase $\theta_{h_{SR}}$ still yields a uniformly distributed phase; and ii) $\mathrm{J}_0(\cdot)$ denotes the zero-order Bessel function of the first kind.

Substituting (51) and (50) in (49), we obtain:

$$\begin{aligned}&\mathrm{APEP}_{\mathrm{NI}}^{(SR)}\left(x_S^{(R)}(t)\to\widetilde{x}_S^{(R)}(t)\right)\\&=\frac{1}{\pi}\int_0^{\infty}\mathcal{F}_{|h_{SR}|}(\omega)\exp\left(-(1/4)N_0\omega^2\right)\\&\times\left(1-\exp\left(-(1/2)E_R|x_R(t)|^2\sigma_{RR}^2\omega^2\right)\right.\\&\left.\times\mathrm{J}_0\left(\sqrt{E_R}|x_R(t)|\mu_{RR}\omega\right)\right)\end{aligned}\tag{52}$$

where $\mathcal{F}_{|h_{SR}|}(\omega)$ is given as follows:

$$\begin{aligned}&\mathcal{F}_{|h_{SR}|}(\omega)=\mathbb{E}_{|h_{SR}|}\left\{\sin\left((1/2)\sqrt{E_S}|h_{SR}|\left|\Delta_S^{(R)}(t)\right|\omega\right)\right\}\\&=\int_0^{\infty}\sin\left((1/2)\sqrt{E_S}|h_{SR}|\left|\Delta_S^{(R)}(t)\right|\omega\right)f_{|h_{SR}|}(x)\,dx\\&\overset{(a)}{=}\frac{\sqrt{\pi}\sqrt{E_S}\sigma_{SR}\left|\Delta_S^{(R)}(t)\right|\omega}{4}\exp\left(-\frac{E_S\sigma_{SR}^2\left|\Delta_S^{(R)}(t)\right|^2\omega^2}{16}\right)\end{aligned}\tag{53}$$

where: i) $f_{|h_{SR}|}(x)=\left(2x/\sigma_{SR}^2\right)\exp\left(-x^2/\sigma_{SR}^2\right)$ denotes the PDF of $|h_{SR}|$, which is Rayleigh distributed; and ii) (a) follows from [65, 3.952].

Finally, the expression of $\mathrm{APEP}_{\mathrm{NI}}^{(SR)}\left(x_S^{(R)}(t)\to\widetilde{x}_S^{(R)}(t)\right)$ in (14) follows by inserting (53) in (52), and then subsequently solving the integral in (52) using [65, 6.631] and with the aid of some simplifications. This concludes the proof.

APPENDIX II
PROOF OF PROPOSITION I

Based on (36) and (37), the condition where SM-FDR shows equal or better performance in terms of achievable rate than SM-HDR can be formulated as follows:

$$\begin{aligned}&\mathcal{C}_{\mathrm{SM-FDR}}\geq\mathcal{C}_{\mathrm{SM-HDR}}\\&\log_2\left(1+\mathcal{G}_{\mathrm{SM-HDR}}^{(SR)}\right)\\&\quad\geq\log_2\left(1+\sqrt{1+\min\left\{\mathcal{G}_{\mathrm{SM-HDR}}^{(SR)},\mathcal{G}_{\mathrm{SM-HDR}}^{(SRD)}\right\}}-1\right)\end{aligned}\tag{54}$$

Again, from (36) and (37) it follows that the condition in (54) is equivalent to the following:

$$\begin{aligned}&\frac{1}{N_R}\sum_{p=1}^{N_R}\sum_{\substack{r=1\\r\neq p}}^{N_R}\frac{(E_S/N_0)|h_{SR_r}|^2}{(E_R/N_0)\left|h_{R_pR_r}\right|^2+1}\geq\mathcal{T}_{\mathrm{SM-HDR}}\\&\sum_{p=1}^{N_R}\sum_{\substack{r=1\\r\neq p}}^{N_R}\frac{1}{(E_R/N_0)\left|h_{R_pR_r}\right|^2+1}\overset{(a)}{\geq}\frac{N_R\overline{\mathcal{T}}_{\mathrm{SM-HDR}}}{\overline{\gamma}_{SR}}\\&(E_R/N_0)^{1-\lambda^*}\overset{(b)}{\leq}-1+\frac{2(N_R-1)\overline{\gamma}_{SR}(1+K_{RR})}{\overline{\mathcal{T}}_{\mathrm{SM-HDR}}(2+K_{RR})}\\&1-\lambda^*\leq\frac{\ln\left(-1+\frac{2(N_R-1)\overline{\gamma}_{SR}(1+K_{RR})}{\overline{\mathcal{T}}_{\mathrm{SM-HDR}}(2+K_{RR})}\right)}{\ln(E_R/N_0)}\\&\lambda^*\geq1-\frac{\ln\left(-1+\frac{2(N_R-1)\overline{\gamma}_{SR}(1+K_{RR})}{\overline{\mathcal{T}}_{\mathrm{SM-HDR}}(2+K_{RR})}\right)}{\ln(E_R/N_0)}\end{aligned}\tag{55}$$

where: i) $\mathcal{T}_{\mathrm{SM-HDR}}=\sqrt{1+\min\left\{\mathcal{G}_{\mathrm{SM-HDR}}^{(SR)},\mathcal{G}_{\mathrm{SM-HDR}}^{(SRD)}\right\}}-1$; ii) $\overline{\mathcal{T}}_{\mathrm{SM-HDR}}=\mathbb{E}_{\mathbf{h}_{\mathcal{T}_{\mathrm{SM-HDR}}}}\{\mathcal{T}_{\mathrm{SM-HDR}}\}$, with $\mathbf{h}_{\mathcal{T}_{\mathrm{SM-HDR}}}$ being the short-hand used to denote all fading channels in the expression of $\mathcal{T}_{\mathrm{SM-HDR}}$; iii) (a) follows by taking the expectation with respect to h_{SR_r}, and by assuming $\overline{\gamma}_{SR}=\overline{\gamma}_{SR_r}$, for $r=1,2,...,N_R$; and iv) (b) follows with the aid of (2), and by assuming $K_{R_pR_r}=K_{RR}$, for $p,r\in\{1,2,...,N_R\}$, with $p\neq r$. Other inequalities in (55) follow from trivial mathematical manipulations. Thus, (38) is obtained, and this concludes the proof.

REFERENCES

[1] J. N. Laneman, D. Tse, and G. W. Wornell, "Cooperative diversity in wireless networks: Efficient protocols and outage behavior", *IEEE Trans. Inform. Theory*, vol. 50, no. 12, pp. 3062-3080, Dec. 2004.

[2] S. W. Peters, A. Y. Panah, K. T. Truong, and R. W. Heath Jr., "Relay architectures for 3GPP LTE-advanced", *EURASIP J. Wireless Commun. and Networking*, vol. 2009, 14 pages, July 2009.

[3] A. Nosratinia, T. E. Hunter, and A. Hedayat, "Cooperative communications in wireless networks", *IEEE Commun. Mag.*, vol. 42, no. 10, pp. 74-80, Oct. 2004.

[4] Z. Ding, Member, I. Krikidis, B. Rong, J. S. Thompson, C. Wang, and S. Yang, "On combating the half-duplex constraint in modern cooperative networks: Protocols and techniques", *IEEE Wireless Commun. Mag.*, vol. 19, no. 6, pp. 20-27, Jun. 2012.

[5] R. U. Nabar, H. Bolcskei, and F. W. Kneubuhler, "Fading relay channels: Performance limits and space-time signal designs", *IEEE J. Sel. Areas Commun.*, vol. 22, no. 6, pp. 1099-1109, Aug. 2004.

[6] K. Azarian, H. El Gamal, and P. Schniter, "On the achievable diversity-multiplexing tradeoff in half-duplex cooperative channels", *IEEE Trans. Inform. Theory*, vol. 51, no. 12, pp. 4152-4172, Dec. 2005.

[7] S. Yang and J.-C. Belfiore, "Optimal space-time codes for the MIMO amplify-and-forward cooperative channel", *IEEE Trans. Inform. Theory*, vol. 53, no. 2, pp. 647-663, Feb. 2007.

[8] Y. Fan, C. Wang, J. S. Thompson, and H. V. Poor, "Recovering multiplexing loss through successive relaying using repetition coding", *IEEE Trans. Wireless Commun.*, vol. 6, no. 12, pp. 4484-4493, Dec. 2007.

$$\begin{aligned}&\mathrm{APEP}_{\mathrm{NI}}^{(SR)}\left(x_S^{(R)}(t)\to\widetilde{x}_S^{(R)}(t)\right)=\mathbb{E}_{|h_{SR}|,\theta_{h_{SR}},\overline{h}_{RR},\overline{n}_R}\left\{\mathrm{PEP}_{\mathrm{NI}}^{(SR)}\left(x_S^{(R)}(t)\to\widetilde{x}_S^{(R)}(t)\,|\,|h_{SR}|,\theta_{h_{SR}},\overline{h}_{RR},\overline{n}_R\right)\right\}\\&=\mathbb{E}_{|h_{SR}|,\theta_{h_{SR}},\overline{h}_{RR},\overline{n}_R}\left\{\frac{1}{\pi}\int_0^{\infty}\sin\left((1/2)\sqrt{E_S}|h_{SR}|\left|\Delta_S^{(R)}(t)\right|\omega\right)\omega^{-1}\Phi_{\overline{n}_R}(\omega)\left(1-\Phi_{\overline{I}_R}(\omega)\right)d\omega\right\}\end{aligned}\tag{49}$$

[9] C. Wang, Y. Fan, J. S. Thompson, M. Skoglund, and H. V. Poor "Approaching the optimal diversity-multiplexing tradeoff in a four-node cooperative network", *IEEE Trans. Wireless Commun.*, vol. 9, no. 12, pp. 3690-3700, Dec. 2010.

[10] S. Zhang, S. Liew, and P. Lam, "Physical layer network coding", *ACM MobiCom*, pp. 358-365, Sep. 2006.

[11] S. Katti, S. Gollakota, and D. Katabi, "Embracing wireless interference: Analog network coding", *ACM SIGCOMM*, pp. 397-408, Oct. 2007.

[12] E. G. Larsson and B. R. Vojcic, "Cooperative transmit diversity based on superposition modulation", *IEEE Commun. Lett.*, vol. 9, vol. 9, pp. 778-780, Sep. 2005.

[13] I. Krikidis, "Analysis and optimization issues for superposition modulation in cooperative networks", *IEEE Trans. Veh. Tech.*, vol. 58, pp. 4837-4847, Nov. 2009.

[14] S. Narayanan, M. Di Renzo, F. Graziosi, and H. Haas, "Distributed Spatial Modulation for Relay Networks", *IEEE Veh. Technol. Conf.-Fall*, pp. 1-6, Sep. 2013.

[15] S. Narayanan, M. Di Renzo, F. Graziosi, and H. Haas, "Distributed Spatial Modulation: A Cooperative Diversity Protocol for Half-Duplex Relay-Aided Wireless Networks", *IEEE Trans. Veh. Technol.*, vol. 65, no. 5, pp. 2947-2964, May 2016.

[16] D. Bharadia and S. Katti, "Full duplex MIMO radios", *ACM USENIX*, pp. 1-13, Apr. 2014.

[17] M. Jain et al., "Practical, Real Time Full Duplex Wireless", *ACM MOBICOM*, pp. 301–312 2011, Sept. 2011.

[18] S. Hong et al., "Applications of self-interference cancellation in 5G and beyond" *IEEE Commun. Mag.*, vol. 52, no. 2, pp. 114-121, Feb. 2014.

[19] Z. Zhang, X. Chai, K. Long, A. V. Vasilakos and L. Hanzo, "Full duplex techniques for 5G networks: self-interference cancellation, protocol design, and relay selection", *IEEE Commun. Mag.*, vol. 53, no. 5, pp. 128-137, May 2015.

[20] A. Sabharwal, P. Schniter, D. Guo, D. Bliss, S. Rangarajan, and R. Wichman, "In-band full-duplex wireless: Challenges and opportunities", *IEEE J. Sel. Areas Commun.*, vol. 32, no. 9, pp. 1637-1652, Sep. 2014.

[21] L. Jimnez Rodrguez, N. H. Tran and T. Le-Ngoc, "Performance of Full-Duplex AF Relaying in the Presence of Residual Self-Interference", *IEEE J. Sel. Areas Commun.*, vol. 32, no. 9, pp. 1752-1764, Sept. 2014.

[22] D. S. Michalopoulos, J. Schlenker, J. Cheng and R. Schober, "Error rate analysis of full-duplex relaying", *Waveform Diversity and Design Conf.*, pp. 165-168, 2010

[23] I. Krikidis, H. Suraweera, S. Yang, and K. Berberidis, "Full-duplex relaying over block fading channel: A diversity perspective", *IEEE Trans. Wireless Commun.*, vol. 11, no. 12, pp. 4524-4535, Dec. 2012.

[24] M. G. Khafagy, A. Ismail, M. S. Alouini and S. Assa, "Efficient Cooperative Protocols for Full-Duplex Relaying Over Nakagami-m Fading Channels", *IEEE Trans. Wireless Commun.*, vol. 14, no. 6, pp. 3456-3470, June 2015.

[25] I. Krikidis and H.A. Suraweera, "Full-Duplex Cooperative Diversity with Alamouti Space-Time Code", *IEEE Wireless Commun. Lett.*, vol. 2, no. 5, pp. 519-522, October 2013.

[26] T. Riihonen, S. Werner, and R. Wichman, "Hybrid full-duplex/halfduplex relaying with transmit power adaptation", *IEEE Trans. Wireless Commun.*, vol. 10, no. 9, pp. 3074-3085, Sep. 2011.

[27] T. Kwon, S. Lim, S. Choi and D. Hong, "Optimal Duplex Mode for DF Relay in Terms of the Outage Probability", *IEEE Trans. Veh. Technol.*, vol. 59, no. 7, pp. 3628-3634, Sept. 2010.

[28] I. Krikidis, H. A. Suraweera, P. J. Smith and C. Yuen, "Full-Duplex Relay Selection for Amplify-and-Forward Cooperative Networks", *IEEE Trans. Wireless Commun.*, vol. 11, no. 12, pp. 4381-4393, December 2012.

[29] R. Y. Mesleh, H. Haas, S. Sinanovic, C. W. Ahn, and S. Yun, "Spatial modulation", *IEEE Trans. Veh. Technol.*, vol. 57, no. 4, pp. 2228-2241, July 2008.

[30] M. Di Renzo, H. Haas, A. Ghrayeb, S. Sugiura, and L. Hanzo, "Spatial modulation for generalized MIMO: Challenges, opportunities and implementation", *Proc. of the IEEE*, vol. 102, no. 1, pp. 56–103, Jan. 2014.

[31] M. Di Renzo, H. Haas, P. Grant, "Spatial modulation for multiple-antenna wireless systems - A survey", *IEEE Commun. Mag.*, vol. 49, no. 12, pp. 182–191, Dec. 2011.

[32] M. Maleki, H. R. Bahrami, A. Alizadeh and N. H. Tran, "On the Performance of Spatial Modulation: Optimal Constellation Breakdown", *IEEE Trans. Commun.*, vol. 62, no. 1, pp. 144–157, January 2014.

[33] M. Di Renzo and H. Haas, "Bit error probability of SM-MIMO over generalized fading channels", *IEEE Trans. Veh. Technol.*, vol. 61, no. 3, pp. 1124–1144, Mar. 2012.

[34] M. Di Renzo and H. Haas, "On transmit-diversity for spatial modulation MIMO: Impact of spatial constellation diagram and shaping filters at the transmitter", *IEEE Trans. Veh. Technol.*, vol. 62, no. 6, pp. 2507-2531, July 2013.

[35] M. Di Renzo, D. De Leonardis, F. Graziosi, and H. Haas, "Space shift keying (SSK-) MIMO with practical channel estimates," *IEEE Trans. Commun.*, vol. 60, no. 4, pp. 998-1012, Apr. 2012.

[36] M. Di Renzo and H. Haas, "Bit error probability of space shift keying MIMO over multiple-access independent fading channels," *IEEE Trans. Veh. Technol.*, vol. 60, no. 8, pp. 3694-3711, Oct. 2011.

[37] N. Serafimovski, A. Younis, R. Mesleh, P. Chambers, M. Di Renzo, C.X. Wang, P. M. Grant, M. A. Beach, and H. Haas, "Practical implementation of spatial modulation", *IEEE Trans. Veh. Technol.*, vol. 62, no. 9, pp. 4511-4523, Nov. 2013.

[38] A. Stavridis, S. Sinanovic, M. Di Renzo, H. Haas, and P. M. Grant, "An energy saving base station employing spatial modulation," *IEEE Int. Workshop on Computer-Aided Modeling Analysis and Design of Commun. Links and Networks*, pp. 1-6, Sep. 2012.

[39] P. Patcharamaneepakorn *et al.*, "Spectral, Energy and Economic Efficiency of 5G Multi-cell Massive MIMO Systems with Generalized Spatial Modulation", *IEEE Trans. Veh. Technol.*, vol. 65, no. 12, pp. 9715-9731, Dec. 2016..

[40] S. Narayanan, M. J. Chaudhry, A. Stavridis, M. Di Renzo, F. Graziosi and H. Haas, "Multi-user spatial modulation MIMO", IEEE Wireless Commun. and Networking Conference, pp. 671–676, Apr. 2014

[41] P. Yang, M. Di Renzo, Y. Xiao, S. Li, and L. Hanzo, "Design guidelines for spatial modulation", *IEEE Commun. Surveys and Tuts.*, vol 17, no. 1, pp. 6-26, Mar. 2015.

[42] A. Shehni, S. Narayanan and M. F. Flanagan, "A virtual full duplex distributed spatial modulation technique for relay networks", *IEEE Int. Symp. Pers. Indoor Mobile Radio Commun.*, pp. 1-6, Sep. 2016.

[43] J. Jeganathan, A. Ghrayeb, L. Szczecinski, and A. Ceron, "Space-shift keying modulation for MIMO channels", *IEEE Trans. Wireless Commun.*, vol. 8, no. 7, pp. 3692–3703, July 2009.

[44] S. Narayanan, M. Di Renzo, F. Graziosi, and H. Haas, "Distributed space shift keying for the uplink of relay-aided cellular networks", *IEEE Int. Workshop on Computer-Aided Model. Analysis and Design of Commun. Links and Networks*, pp. 130–134, Sep. 2012.

[45] S. Narayanan, M. Di Renzo, M. J. Chaudhry, F. Graziosi, and H. Haas, "On the Achievable Performance-Complexity Tradeoffs of Relay-Aided Space Shift Keying", *IEEE Trans. Signal and Inf. Processing Over Networks*, vol. 1, no. 2, pp. 129–144, June 2015.

[46] S. Narayanan, A. Stavridis, M. Di Renzo, F. Graziosi, and H. Haas, "Distributed spatially-modulated space-time-block-codes", *IEEE Int. Workshop on Computer-Aided Modeling Analysis and Design of Commun. Links and Networks*, pp. 159-163, Sep. 2013.

[47] S. Sugiura, S. Chen, H. Haas, P. M. Grant, and L. Hanzo, "Coherent versus non–coherent decode–and–forward relaying aided cooperative space–time shift keying", *IEEE Trans. Commun.*, vol. 59, no. 6, pp. 1707–1719, June 2011.

[48] P. Yang, B. Zhang, Y. Xiao, B. Dong, S. Li, M. El–Hajjar, and L. Hanzo, "Detect–and–forward relaying aided cooperative spatial modulation for wireless networks", *IEEE Trans. Commun.*, vol. 61, no. 11, pp. 4500–4511, Nov. 2013.

[49] M. Xu, M. Wen, Y. Feng, F. Ji and W. Pan, "A novel self-interference cancellation scheme for full duplex with differential spatial modulation", *IEEE Int. Symp. Pers. Indoor Mobile Radio Commun.*, pp. 482–486, Sep. 2015.

[50] B. Jiao, M. Wen, M. Ma, H. V. Poor, "Spatial Modulated Full Duplex", *IEEE Wireless Commun. Lett.*, vol. 3, no. 6, pp. 641-644, Dec. 2014.

[51] S. Narayanan, H. Ahmadi and M. F. Flanagan, "Simultaneous Uplink/Downlink Transmission Using Full-Duplex Single-RF MIMO", *IEEE Wireless Commun. Lett.*, vol. 5, no. 1, pp. 88-91, Feb. 2016.

[52] X. Xie, Z. Zhao, M. Peng and W. Wang, "Spatial modulation in two-way network coded channels: Performance and mapping optimization", *IEEE Int. Symp. Pers. Indoor Mobile Radio Commun.*, pp. 72–76, Sep. 2012.

[53] Y. Yang, "Spatial Modulation Exploited in Non-Reciprocal Two-Way Relay Channels: Efficient Protocols and Capacity Analysis", *IEEE Trans. Commun.*, vol. 64, no. 7, pp. 2821–2834, July 2016.

[54] J. Zhang; Q. Li; K. Kim; Y. Wang; X. Ge; J. Zhang, "On the Performance of Full-duplex Two-way Relay Channels with Spatial Modulation", *IEEE Trans. Commun.*, vol. 64, no. 12, pp. 4966-4982, Dec. 2016.

[55] P. Raviteja, Y. Hong and E. Viterbo, "Spatial Modulation in Full-Duplex Relaying", *IEEE Commun. Lett.*, vol. 20, no. 10, pp. 2111–2114, Oct. 2016.

[56] M. Duarte, C. Dick, and A. Sabharwal, "Experiment-driven characterization of full-duplex wireless systems", *IEEE Trans. Wireless Commun.*, vol. 11, no. 12, pp. 4296-4307, Dec. 2012.
[57] G. Auer, V. Giannini, I. Godor, P. Skillermark, M. Olsson, M. Imran, D. Sabella, M. Gonzalez, C. Desset, and O. Blume, "Cellular energy efficiency evaluation framework", *IEEE Veh. Technol. Conf. - Spring*, pp. 1-6, May 2011.
[58] M. K. Simon and M.-S. Alouini, *Digital Communication over Fading Channels*, John Wiley & Sons, 2nd ed., 2005.
[59] Swaminathan R, M. D. Selvaraj and R. Roy, "On the Error and Outage Performance of Decode-and-Forward Cooperative Selection Diversity System With Correlated Links", *IEEE Trans. Veh. Tech.*, vol. 64, no. 8, pp. 3578-3593, Aug. 2015.
[60] J. Gil-Pelaez, "Note on the inversion theorem", *Biometrika*, vol. 38, pp. 481-482, Dec. 1951.
[61] M. Di Renzo and P. Guan, "A Mathematical Framework to the Computation of the Error Probability of Downlink MIMO Cellular Networks by Using Stochastic Geometry", *IEEE Trans. Wireless Commun.*, vol. 62, no. 8, pp. 2860-2879, Aug. 2014.
[62] N. C. Beaulieu and J. Cheng, "Precise error-rate analysis of bandwidth efficient BPSK in Nakagami fading and cochannel interference", *IEEE Trans. Commun.*, vol. 52, no. 1, pp. 149-158, Jan. 2004.
[63] W. Lu, M. Di Renzo, "Performance analysis of Spatial Modulation MIMO in a poisson field of interferers", *IEEE Int. Conf. Comput. Netw. Commun.*, pp. 662-668, Feb. 2014.
[64] E. Biglieri, C. Caire, G. Taricco, and J. Ventura-Traveset, "Computing error probabilities over fading channels: A unified approach", *European Trans. Telecommun.*, vol. 9, no. 1, pp. 15-25, Feb. 1998.
[65] I. S. Gradshteyn and I. M. Ryzhik, *Tables of Integrals, Series, Products*, 7th ed. San Diego, CA, USA: Academic, 2007.
[66] A. Goldsmith, *Wireless Communications*, Cambridge University Press, 2005.
[67] S. S. Ikki and M. H. Ahmed, "Performance Analysis of Decode-and-Forward Incremental Relaying Cooperative-Diversity Networks over Rayleigh Fading Channels", *IEEE Veh. Technol. Conf. - Spring*, pp. 1-6. May 2009.
[68] P. Herhold, E. Zimmermann, G. Fettweis, "A Simple Cooperative Extension to Wireless Relaying", *Int. Zurich Seminar on Commun.*, Zurich, Switzerland, Feb. 2004.
[69] T. Cover and A. El Gamal, "Capacity theorems for the relay channel," *IEEE Trans. Inform. Theory*, vol. 25, no. 5, pp. 572–584, Sep. 1979.
[70] A. Host-Madsen and J. Zhang, "Capacity bounds and power allocation for wireless relay channels," *IEEE Trans. Inform. Theory*, vol. 51, no. 6, pp. 2020–2040, June 2005.
[71] Y. Yang and B. Jiao, "Information-guided channel-hopping for high data rate wireless communication", *IEEE Commun. Lett.*, vol. 12, no. 4, pp. 225-227, Apr. 2008.
[72] R. Rajashekar, K. V. S. Hari, and L. Hanzo, "Reduced-complexity ml detection and capacity-optimized training for spatial modulation systems", *IEEE Trans. Commun.*, vol. 62, no. 1, pp. 112-125, Jan. 2014.
[73] Z. An, J. Wang, J. Wang, S. Huang and J. Song, "Mutual Information Analysis on Spatial Modulation Multiple Antenna System", *IEEE Trans. Commun.*, vol. 63, no. 3, pp. 826-843, Mar. 2015.
[74] I. Krikidis, H. A. Suraweera, P. J. Smith and C. Yuen, "Full-Duplex Relay Selection for Amplify-and-Forward Cooperative Networks", *IEEE Trans. Wireless Commun.*, vol. 11, no. 12, pp. 4381-4393, December 2012.
[75] B. Zhong, D. Zhang, Z. Zhang, Z. Pan, K. Long and A. V. Vasilakos, "Opportunistic full-duplex relay selection for decode-and-forward cooperative networks over Rayleigh fading channels", *IEEE Int. Conf. Commun.*, pp. 5717-5722, June 2014.
[76] B. Yu, L. Yang, X. Cheng and R. Cao, "Power and Location Optimization for Full-Duplex Decode-and-Forward Relaying", *IEEE Trans. Commun.*, vol. 63, no. 12, pp. 4743-4753, Dec. 2015.
[77] NetWorld2020 European Technology Platform for communications networks and services, Feb. 2016. [Online].

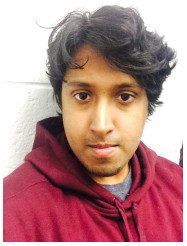

Sandeep Narayanan (M'16) received the B.Tech. degree from Amrita University, India, in 2010, the M.Sc. degree from The University of Edinburgh, UK, in 2011, and the Ph.D. degree in Electrical and Information Engineering from the University of L'Aquila, Italy, in 2015. During the period 2011-2014, he was a Marie-Curie Early Stage Researcher with the Center of Excellence for Research DEWS, University of L'Aquila, and with Wireless Embedded Systems Technologies Aquila s.r.l., Italy. He is currently a research associate with the Centre for Telecommunications Research, King's College London (KCL), UK. Prior to joining KCL, he was a Post-Doctoral Research Fellow with University College Dublin, Ireland. He has also held visiting research positions at Northwestern University, USA, and the University of Edinburgh. His main research interests include wireless communication theory and signal processing.

Hamed Ahmadi (SM'15) is a lecturer at University College Dublin, Ireland. He received his Ph.D. in electrical engineering from National University of Singapore (NUS) in 2012. He worked as a research fellow at CONNECT/CTVR centre, Trinity College Dublin in 2012-2015. Dr. Ahmadi's current research interests include design, analysis, and optimization of wireless communications networks, wireless network virtualization, cognitive radio networks, and the application of machine learning in small cell and self-organizing networks. Dr. Ahmadi is serving several international journals as a reviewer as well as being part of several Technical Programme Committees at different worldwide conferences/congresses. In 2013, Dr. Ahmadi was selected as an exemplary reviewer of IEEE Communications Letters.

Mark F. Flanagan ((M'03-SM'10) received the B.E. and Ph.D. degrees in electronic engineering from University College Dublin, Dublin, Ireland, in 1998 and 2005, respectively.

During 1998-1999, he was a Project Engineer with Parthus Technologies Ltd. Between 2006 and 2008, he held postdoctoral research fellowships with the University of Zurich, Switzerland; the University of Bologna, Italy; and the University of Edinburgh, U.K. In 2008, he was appointed as an SFI Stokes Lecturer in electronic engineering with University College Dublin, where he is currently an Associate Professor. In the summer of 2014, he was a Visiting Senior Scientist with the Institute of Communications and Navigation of the German Aerospace Center, under a DLR-DAAD fellowship. His research interests include information theory, wireless communications, and signal processing.

Dr. Flanagan is currently serving as a Senior Editor for IEEE COMMUNICATIONS LETTERS. He has served on the Technical Program Committees of several IEEE international conferences. He is a Senior Member of the IEEE (Communications and Signal Processing Societies).